IHES 2006
GR Trimester
From Geometry to
Numerics, 20-24 Nov 06

COALESCING BINARY BLACK HOLES

COMPARISON BETWEEN ANALYTICAL AND NUMERICAL RESULTS (MAINLY IN THE EXTREME MASSRATIO LIMIT)

Thibault DAMOUR
IHES

COALESCING BINARY

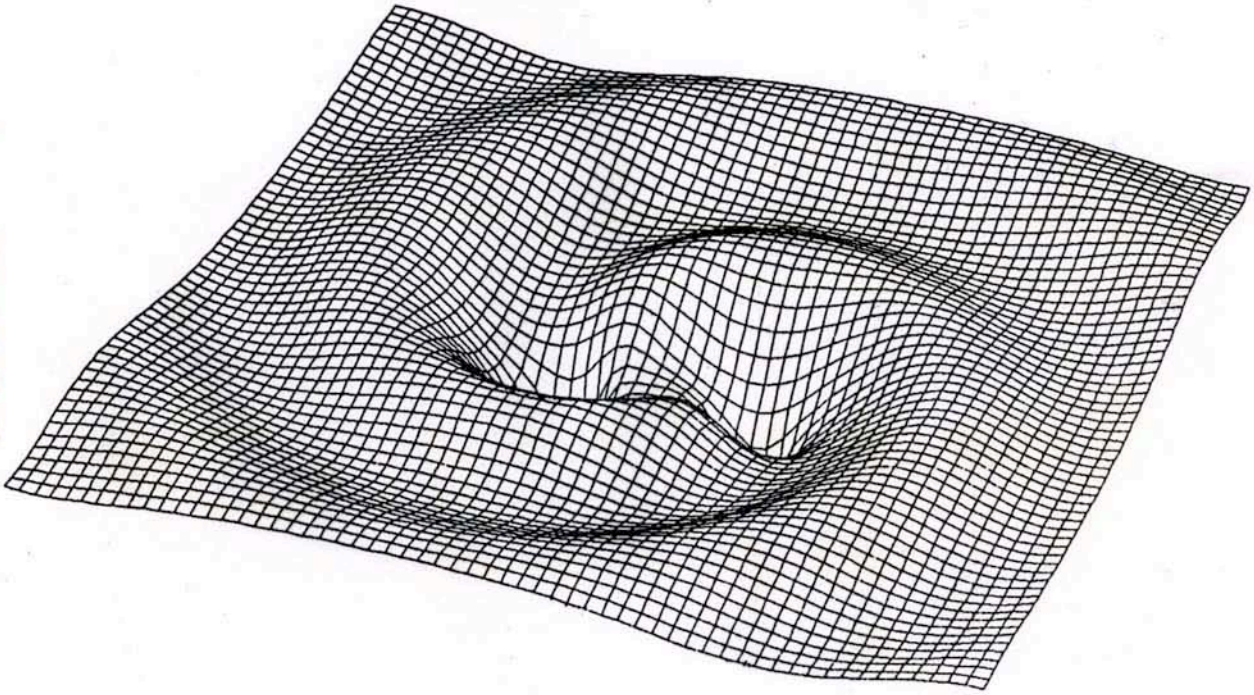

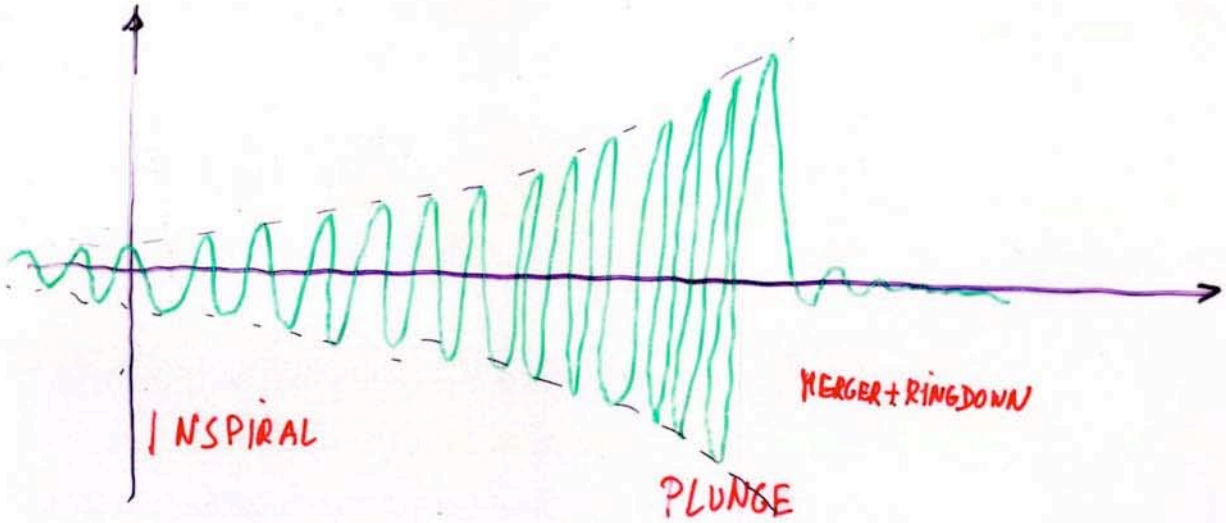

THE PROBLEM

Nice 4.1
S. Thomas 2

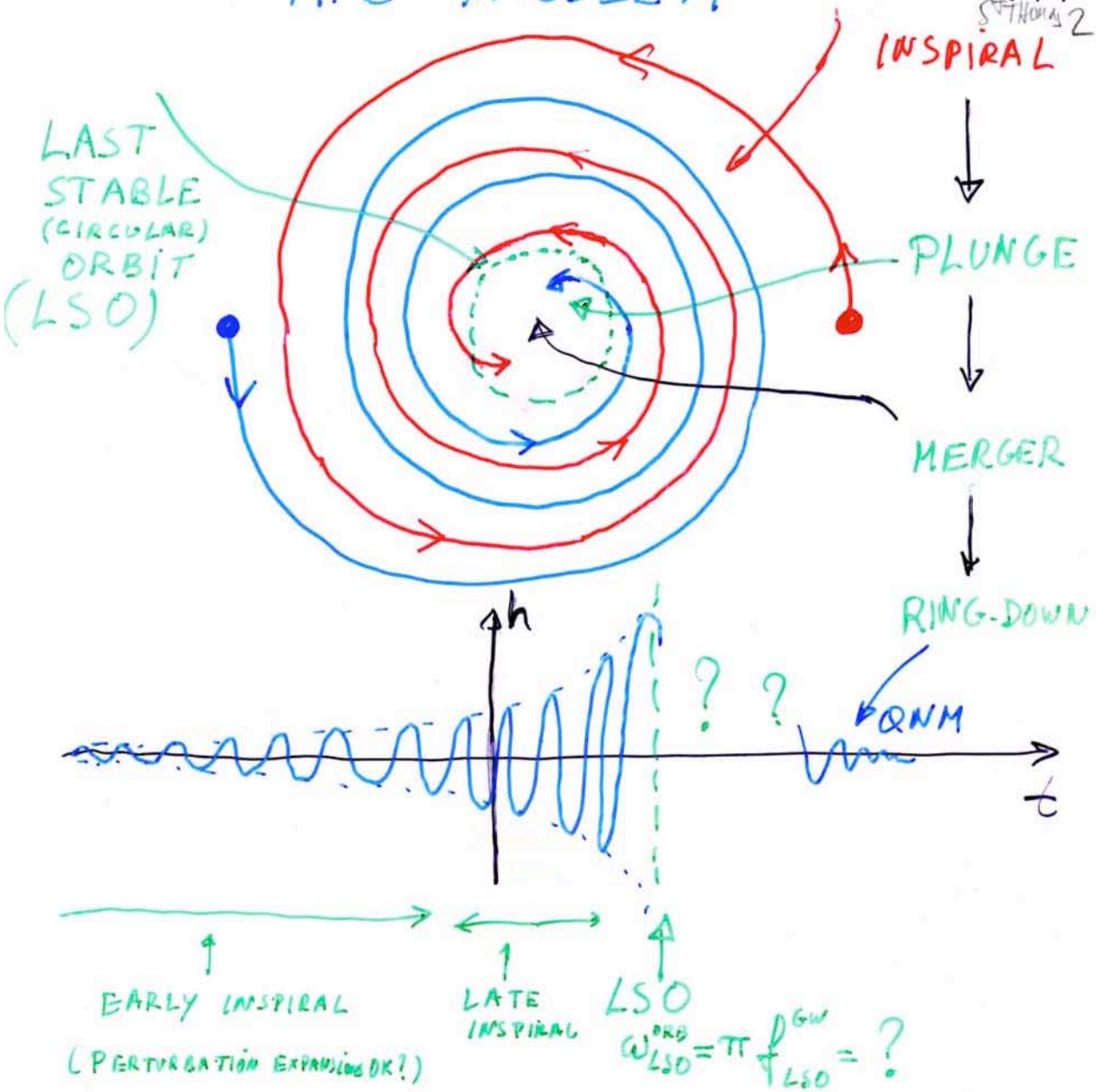

USUAL LORE: "IBBH PROBLEM" (Brady, Creighton, Thorne '98)

CAN USE ANALYTICAL RESULTS (PERTURBATIVE)

MUST USE NUMERICAL RESULTS FOR

LATE INSPIRAL + PLUNGE + MERGER + RING-DOWN

OUR CLAIM

CAN USE ANALYTICAL RESULTS + SOME ROUGH ESTIMATE OF MERGER

BH NS
$(10_{M_\odot}, 1{,}4_{M_\odot})$
SYSTEM

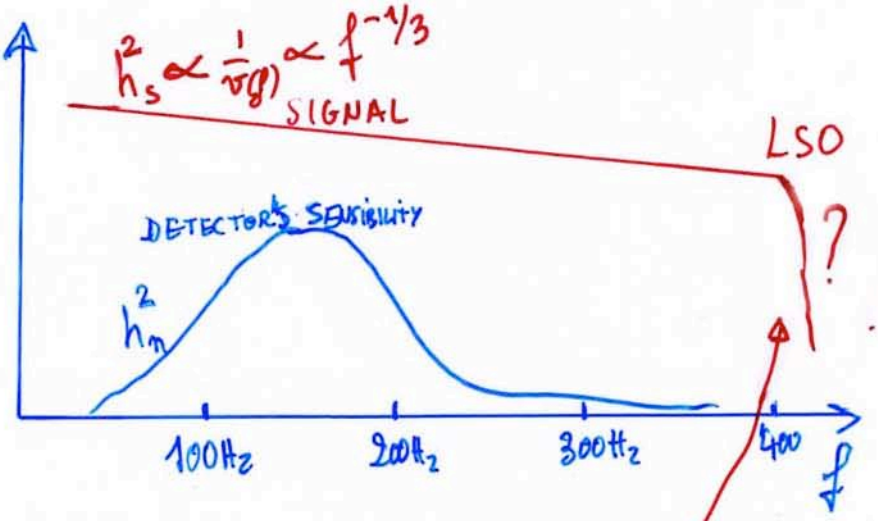

LSO CUT OFF EXPECTED AROUND $F_{LSO} \sim 4400 \frac{M_\odot}{M}$ Hz

BH BH
$(15_{M_\odot}, 15_{M_\odot})$
SYSTEM

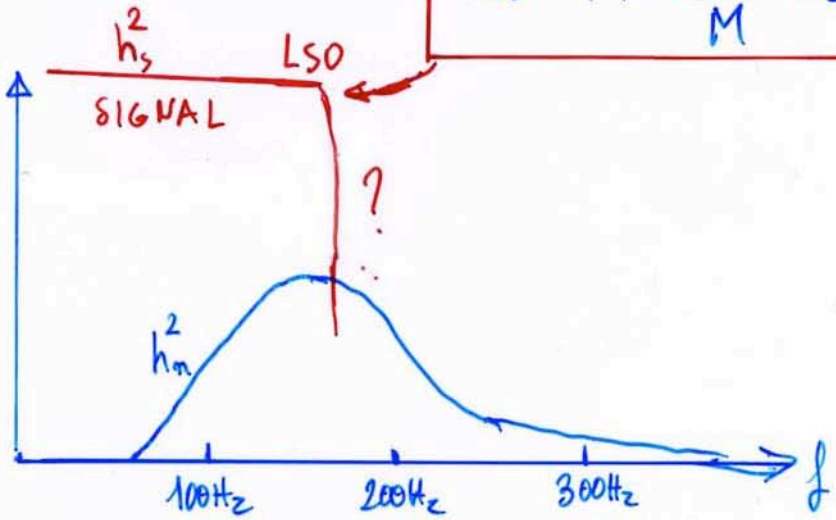

(1.4, 1.4) SYSTEMS : STANDARD PN TEMPLATE WAVEFORMS OK
(10, 1.4)

(10, 10) SYSTEMS : NEED GOOD TEMPLATES AROUND LSO
(15, 15)

CHALLENGES

ANALYTICAL APPROACHES

- NEED EQS OF MOTION TO VERY HIGH PERTURBATION ORDER
- NEED GW GENERATION FORMALISM TO HIGH PERTURBATION ORDER
- NEED TO PACKAGE THIS PERTURBATIVE INFORMATION IN A FORM WHICH REMAINS VALID DURING BOTH INSPIRAL AND PLUNGE, AND WHICH CAN CONNECT WITH MERGER AND RINGDOWN
- (QUASI-) ANALYTICAL DESCRIPTION IS NEEDED FOR COVERING THE FULL PARAMETER SPACE : $m_1, m_2, \vec{S}_1, \vec{S}_2$, ECCENTRICITY, ...

NUMERICAL APPROACHES

- NEED STABLE CODES
- NEED TO DESCRIBE B. HOLES
- NEED TO EXTRACT GW WAVEFORMS
- LIMITED TO A FEW ORBITS BEFORE MERGER
- LIMITED TO EXPLORING A FEW SAMPLE POINTS IN THE PARAMETER SPACE
- GIVES CRUCIAL NON PERTURBATIVE INFORMATION THAT GOES BEYOND WHAT CAN BE ANALYTICALLY COMPUTED

COMPLEMENTARITY

AIM : TAKE ADVANTAGE OF FLEXIBILITY OF ANALYTICAL METHODS, NOTABLY OF RESUMMED (EFFECTIVE ONE BODY + PADÉ) PN METHODS, TO CONSTRUCT GW TEMPLATES THAT HAVE A GOOD PHASING ALL OVER INSPIRAL + PLUNGE + MERGER + RINGDOWN

TOOL : COMPARISON BETWEEN EOB-LIKE TEMPLATES/PREDICTIONS AND NUMERICAL RESULTS

- $\nu \equiv \frac{m_1 m_2}{(m_1+m_2)^2} \sim \frac{1}{4}$ COMPARABLE MASSES
- OR $\nu \ll 1$ EXTREME MASS RATIO

'RESTRICTED' WAVE FORM

$h(t) \equiv v_\omega^2 \cos 2\varphi(t)$

$v_\omega = (\dot{\varphi})^{1/3}$

(Buonanno, Damour '00)

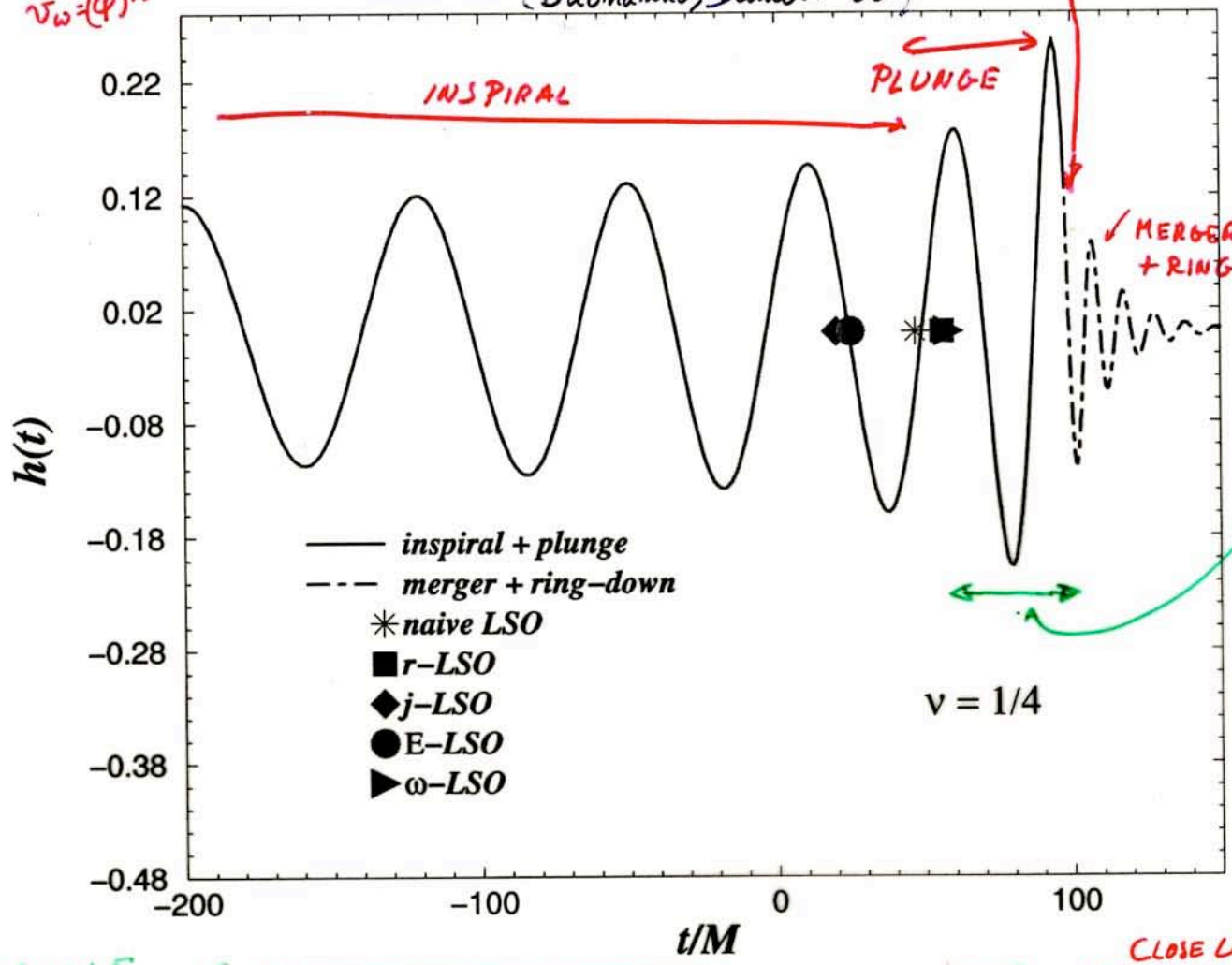

MATCHING TO LEAST-DAMPED QUASI-NORMAL-MODE OF A KERR BH (WITH $M = E^{\text{light-ring}}$, $J = J^{\text{light-ring}}$) AT THE (v-DEFORMED) LIGHT-RING

ONLY 1.2 GW PERIOD DURING PLUNGE ($\sim 6M \to \sim 3M$)

T1816 Nice 4.25

POSSIBLE FUTURE IMPROVEMENTS

HIGHER PERTURBATIVE ACCURACY in H and $\mathcal{F}$

CLOSE LIMIT APPROXIMATION

Smarr, Bowe, Pullin ...

recently: Baker et al '01

NUMERICAL CALC.

BH initial data: Cook; Baumgarte, Grandclement et al

Baker et al. 106

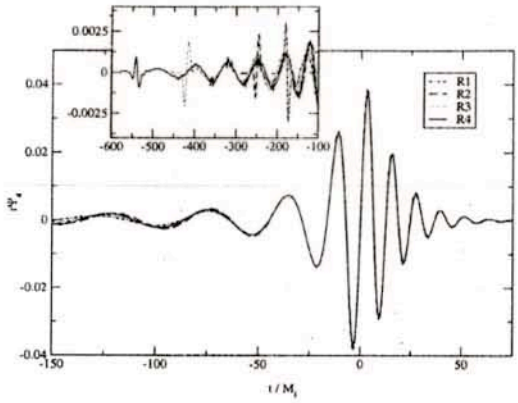

FIG. 5: Waveforms from runs R1 - R4. The figure shows nearly perfect agreement after $t = -50M_f$. For the preceding $500M_f$, shown in an inset, the waveforms agree in phase and amplitude within about 10% except for a brief initial pulse at the beginning of each run.

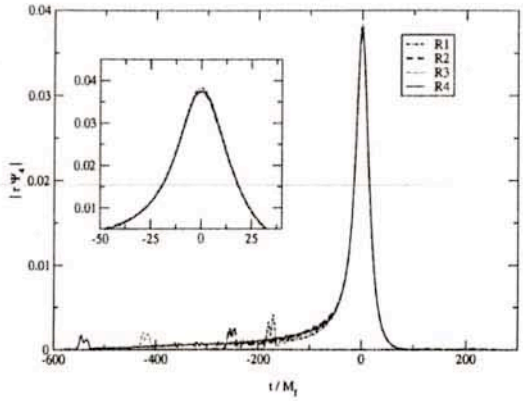

FIG. 6: Amplitudes, absolute value of (complex) Ψ_4, of the waves. The curves have been shifted such that the maxima are all at time 0. The inset zooms into the peak showing the strong agreement from $t = -50M_f$ on. We have used the amplitude peak as a reference to align our simulations in time.

nary system in our simulations. Following the discussion in Sec. IV, we measure the radiation energy extracted at $r_{ex} = 30M$, estimating that these will be accurate within $\sim 1\%$. We subtract the radiation energy E_{rad} from the initial mass M_0, given in Table I, to determine the final black hole mass in each simulation, $M_f = M_0 - E_{rad}$. This provides a physical scaling which we use to compare the R1-R4 simulations. Similarly, we measure the angular momentum content of the radiation J_{rad} as extracted at $r_{ex} = 50M$, estimating the accuracy to be within a few percent. Subtracting this from the initial ADM angular momentum J_0, we calculate the spin parameter of the final black hole $a/M_f = (J_0 - J_{rad})/M_f^2$. The results are summarized in Table V.

	E_{rad}/M_f	J_{rad}/M_f^2	a/M_f	M_{QN}/M_f	a_{QN}/M_f
R1	0.0356	0.246	0.694	1.005	0.721
R2	0.0369	0.272	0.691	1.002	0.686
R3	0.0381	0.306	0.689	1.004	0.694
R4	0.0387	0.325	0.702	1.004	0.693

TABLE V: Energy and angular momenta for the radiation and final black hole. E_{rad} and J_{rad} are measured at $r_{ex} = 30M$, and $r_{ex} = 50M$, respectively. M_{QN} and a_{QN} are calculated independently from the quasi-normal fits of the ringdown waveforms, and agree well with the values deduced from the radiative losses.

We note that the energy and angular momentum content of the radiation is almost entirely contained in the $l = 2, m = \pm 2$ spin -2-weighted spherical harmonic components, with other components entering at the 1% level. In the remainder of our waveform analysis we concentrate exclusively on the leading component,

$$r\psi_4(\theta,\varphi) \sim r\Psi_{4\,(22)}\,({}_{-2}Y_{2\,2}(\theta,\phi) + {}_{-2}Y_{2\,-2}(\theta,\phi)) \quad (4)$$

where, for simplicity, we have suppressed retarded time dependence. Hereafter we suppress the multipole labels and refer to the leading component simply as $r\Psi_4$. The two polarization components of the radiation are represented in the real and imaginary parts of $r\Psi_4$. We follow Refs. [14, 25], representing our waveforms by $r\Psi_4 = A\exp(-i\varphi_{pol})$, where the amplitude A and polarization phase φ_{pol}, like $r\Psi_4$, are functions of time. Of course, any complex time-series could be represented in this form, but it is particularly valuable if the radiation exhibits a *circular polarization* pattern, so that A and φ_{pol} vary slowly compared to the wave frequency timescale. Such radiation will be circularly polarized to an observer on the system's rotational axis, varying to linearly polarization for an observer on the equatorial plane. We find that the radiation produced in our simulations shows strong circular polarization, which we will utilize in comparing the radiation from our four simulations.

As we are interested in the degree to which our various runs may be taken to be different models of the same physical merger spacetime, we must define a physical basis for comparing them. As expected, runs beginning with more separated black holes take a longer time to reach the point of merger. For each run, a physical reference time is recognizable by the point at which the radiation reaches its peak amplitude; we define $t = 0$ at this point for our comparisons.

Fig. 6 shows the wave amplitudes $A(t)$ from all four runs. Through the strong radiation peak after $t = -50M_f$ all four wave amplitudes show striking universality in the compared results, with agreement among all runs to about 1%. This period of strong agreement covers roughly the last orbit, plunge and ringdown of the merger. Agreement within about 10% is maintained among the R2-R4 simulations for most of each run with

WHAT IS NEEDED FOR DESCRIBING COALESCING BINARIES

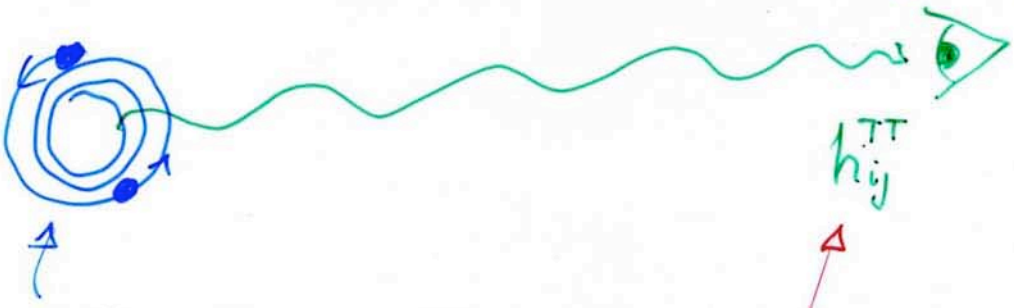

$$\text{E o M} \quad a=1,2 \qquad \frac{d^2\vec{x}_a}{dt^2} = \vec{a}_a^{\,CONS} + \vec{a}_a^{\,RR}$$

$$r h_{ij}^{TT} = \left[U_{ij} + U_{ijk}\frac{N^k}{c} + \cdots \right]^{TT}$$

NEED RADIATION REACTION TO HIGHEST POSSIBLE ACCURACY

$$a^{RR} = \frac{GM}{r^2}\left[\frac{v^5}{c^5} + \frac{v^7}{c^7} + \underbrace{\frac{v^8}{c^8} + \frac{v^9}{c^9} + \frac{v^{10}}{c^{10}} + \frac{v^{11}}{c^{11}} + \frac{v^{12}}{c^{12}}}_{\text{HEURISTICALLY OBTAINED BY ASSUMING BALANCE OF } E,\ \vec{J}} \right]$$

WAVE FORM :

$$U_{ij} = p\langle x^i x^j \rangle \left\{ 1 + \frac{v^2}{c^2} + \frac{v^3}{c^3} + \frac{v^4}{c^4} + \frac{v^5}{c^5} + \frac{v^6}{c^6} + \frac{v^7}{c^7} \right\}$$

\+ NEED CONSERVATIVE DYNAMICS TO HIGHEST POSSIBLE ACCURACY

$$a^{CONS} = \frac{GM}{r^2}\left[1 + \frac{v^2}{c^2} + \frac{v^4}{c^4} + \frac{v^6}{c^6} \right]$$

OR

$$H[x,p] = H_0 + \frac{1}{c^2}H_2 + \frac{1}{c^4}H_4 + \frac{1}{c^6}H_6$$

HIGH-PERTURBATION ORDER CALCULATIONS OF EQS. OF MOTION

- REPLACE 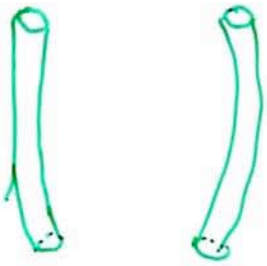 BY 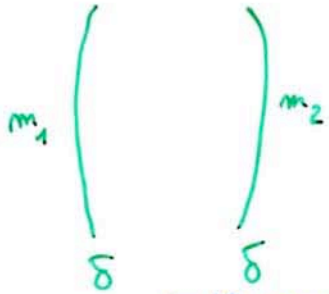

BECAUSE OF EFFACEMENT OF INTERNAL STRUCTURE UP TO $\left(\frac{v}{c}\right)^{10}$ ~ 5PN ORDER (Damour, '82)

- CONSERVATIVE PART OF HAMILTONIAN :

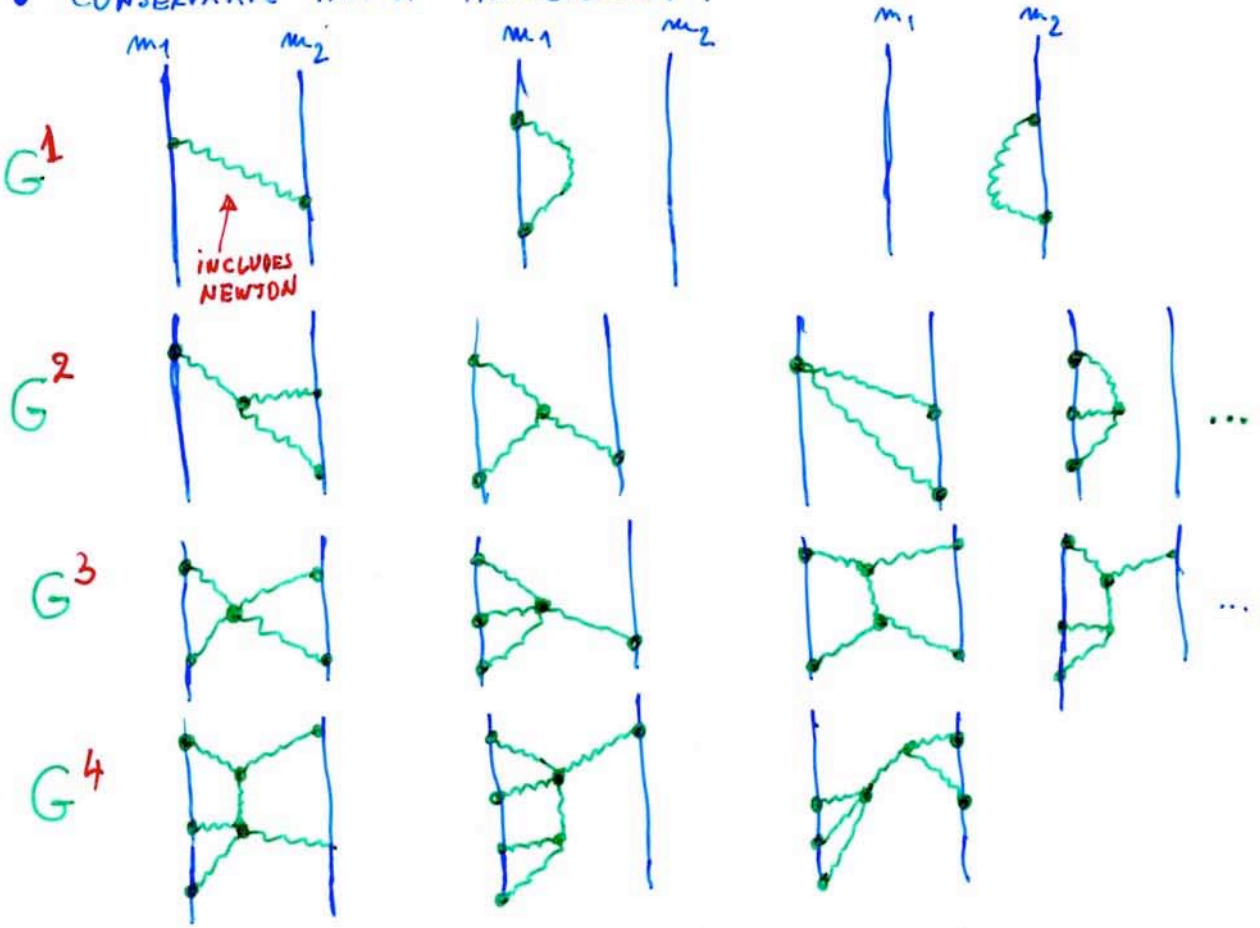

- NEED DIMENSIONAL REGULARIZATION ('t Hooft Veltman '72) TO COMPUTE G^4 (3PN ~ 3 LOOP) (Damour Jaranowski Schäfer '00, Blanchet Damour Esposito F. '04)
  - in ADM FORMALISM
  - HARMONIC GAUGE

3PN HAMILTONIAN (Damour, Jaranowski, Schäfer 100)

$$H(\mathbf{x}_a,\mathbf{p}_a)=\sum_a m_a c^2+H_{\rm N}(\mathbf{x}_a,\mathbf{p}_a)+\frac{1}{c^2}H_{\rm 1PN}(\mathbf{x}_a,\mathbf{p}_a)+\frac{1}{c^4}H_{\rm 2PN}(\mathbf{x}_a,\mathbf{p}_a)+\frac{1}{c^6}H_{\rm 3PN}(\mathbf{x}_a,\mathbf{p}_a)+\mathcal{O}\left(\frac{1}{c^8}\right). \tag{5}$$

At the Newtonian order, i.e. when keeping the rest-mass term $\Sigma_a m_a c^2$ and the Newtonian-level Hamiltonian,

$$H_{\rm N}(\mathbf{x}_a,\mathbf{p}_a)=\sum_a\frac{\mathbf{p}_a^2}{2\,m_a}-\frac{1}{2}\sum_a\sum_{b\neq a}\frac{G\,m_a\,m_b}{r_{ab}}, \tag{6}$$

$$H_{\rm 1PN}(\mathbf{x}_a,\mathbf{p}_a)=-\frac{1}{8}\frac{(\mathbf{p}_1^2)^2}{m_1^3}+\frac{1}{8}\frac{Gm_1m_2}{r_{12}}\left[-12\frac{\mathbf{p}_1^2}{m_1^2}+14\frac{(\mathbf{p}_1\cdot\mathbf{p}_2)}{m_1m_2}+2\frac{(\mathbf{n}_{12}\cdot\mathbf{p}_1)(\mathbf{n}_{12}\cdot\mathbf{p}_2)}{m_1m_2}\right]$$
$$+\frac{1}{4}\frac{Gm_1m_2}{r_{12}}\frac{G(m_1+m_2)}{r_{12}}+(1\longleftrightarrow 2),$$

$$H_{\rm 2PN}(\mathbf{x}_a,\mathbf{p}_a)=\frac{1}{16}\frac{(\mathbf{p}_1^2)^3}{m_1^5}+\frac{1}{8}\frac{Gm_1m_2}{r_{12}}\left[5\frac{(\mathbf{p}_1^2)^2}{m_1^4}-\frac{11}{2}\frac{\mathbf{p}_1^2\mathbf{p}_2^2}{m_1^2m_2^2}-\frac{(\mathbf{p}_1\cdot\mathbf{p}_2)^2}{m_1^2m_2^2}+5\frac{\mathbf{p}_1^2(\mathbf{n}_{12}\cdot\mathbf{p}_2)^2}{m_1^2m_2^2}\right.$$
$$\left.-6\frac{(\mathbf{p}_1\cdot\mathbf{p}_2)(\mathbf{n}_{12}\cdot\mathbf{p}_1)(\mathbf{n}_{12}\cdot\mathbf{p}_2)}{m_1^2m_2^2}-\frac{3}{2}\frac{(\mathbf{n}_{12}\cdot\mathbf{p}_1)^2(\mathbf{n}_{12}\cdot\mathbf{p}_2)^2}{m_1^2m_2^2}\right]$$
$$+\frac{1}{4}\frac{G^2m_1m_2}{r_{12}^2}\left[m_2\left(10\frac{\mathbf{p}_1^2}{m_1^2}+19\frac{\mathbf{p}_2^2}{m_2^2}\right)-\frac{1}{2}(m_1+m_2)\frac{27(\mathbf{p}_1\cdot\mathbf{p}_2)+6(\mathbf{n}_{12}\cdot\mathbf{p}_1)(\mathbf{n}_{12}\cdot\mathbf{p}_2)}{m_1m_2}\right]$$
$$-\frac{1}{8}\frac{Gm_1m_2}{r_{12}}\frac{G^2(m_1^2+5m_1m_2+m_2^2)}{r_{12}^2}+(1\longleftrightarrow 2).$$

$$H_{\rm 3PN}^{\rm reg}(\mathbf{x}_a,\mathbf{p}_a)=-\frac{5}{128}\frac{(\mathbf{p}_1^2)^4}{m_1^7}+\frac{1}{32}\frac{Gm_1m_2}{r_{12}}\left[-14\frac{(\mathbf{p}_1^2)^3}{m_1^6}+4\frac{\big((\mathbf{p}_1\cdot\mathbf{p}_2)^2+4\mathbf{p}_1^2\mathbf{p}_2^2\big)\mathbf{p}_1^2}{m_1^4m_2^2}+\frac{(\mathbf{p}_1^2\mathbf{p}_2^2-2(\mathbf{p}_1\cdot\mathbf{p}_2)^2)(\mathbf{p}_1\cdot\mathbf{p}_2)}{m_1^3m_2^3}\right.$$
$$-10\frac{\big(\mathbf{p}_1^2(\mathbf{n}_{12}\cdot\mathbf{p}_2)^2+\mathbf{p}_2^2(\mathbf{n}_{12}\cdot\mathbf{p}_1)^2\big)\mathbf{p}_1^2}{m_1^4m_2^2}+24\frac{\mathbf{p}_1^2(\mathbf{p}_1\cdot\mathbf{p}_2)(\mathbf{n}_{12}\cdot\mathbf{p}_1)(\mathbf{n}_{12}\cdot\mathbf{p}_2)}{m_1^4m_2^2}+2\frac{\mathbf{p}_1^2(\mathbf{p}_1\cdot\mathbf{p}_2)(\mathbf{n}_{12}\cdot\mathbf{p}_2)^2}{m_1^3m_2^3}$$
$$+\frac{\big(7\mathbf{p}_1^2\mathbf{p}_2^2-10(\mathbf{p}_1\cdot\mathbf{p}_2)^2\big)(\mathbf{n}_{12}\cdot\mathbf{p}_1)(\mathbf{n}_{12}\cdot\mathbf{p}_2)}{m_1^3m_2^3}+6\frac{\mathbf{p}_1^2(\mathbf{n}_{12}\cdot\mathbf{p}_1)^2(\mathbf{n}_{12}\cdot\mathbf{p}_2)^2}{m_1^4m_2^2}$$
$$\left.+15\frac{(\mathbf{p}_1\cdot\mathbf{p}_2)(\mathbf{n}_{12}\cdot\mathbf{p}_1)^2(\mathbf{n}_{12}\cdot\mathbf{p}_2)^2}{m_1^3m_2^3}-18\frac{\mathbf{p}_1^2(\mathbf{n}_{12}\cdot\mathbf{p}_1)(\mathbf{n}_{12}\cdot\mathbf{p}_2)^3}{m_1^3m_2^3}+5\frac{(\mathbf{n}_{12}\cdot\mathbf{p}_1)^3(\mathbf{n}_{12}\cdot\mathbf{p}_2)^3}{m_1^3m_2^3}\right]$$
$$+\frac{G^2m_1m_2}{r_{12}^2}\left[\frac{1}{16}(m_1-27m_2)\frac{(\mathbf{p}_1^2)^2}{m_1^4}-\frac{115}{16}m_1\frac{\mathbf{p}_1^2(\mathbf{p}_1\cdot\mathbf{p}_2)}{m_1^3m_2}+\frac{1}{48}m_2\frac{25(\mathbf{p}_1\cdot\mathbf{p}_2)^2+371\mathbf{p}_1^2\mathbf{p}_2^2}{m_1^2m_2^2}\right.$$
$$+\frac{17}{16}\frac{\mathbf{p}_1^2(\mathbf{n}_{12}\cdot\mathbf{p}_1)^2}{m_1^3}-\frac{1}{8}m_1\frac{\big(15\mathbf{p}_1^2(\mathbf{n}_{12}\cdot\mathbf{p}_2)+11(\mathbf{p}_1\cdot\mathbf{p}_2)(\mathbf{n}_{12}\cdot\mathbf{p}_1)\big)(\mathbf{n}_{12}\cdot\mathbf{p}_1)}{m_1^3m_2}+\frac{5}{12}\frac{(\mathbf{n}_{12}\cdot\mathbf{p}_1)^4}{m_1^3}$$
$$-\frac{3}{2}m_1\frac{(\mathbf{n}_{12}\cdot\mathbf{p}_1)^3(\mathbf{n}_{12}\cdot\mathbf{p}_2)}{m_1^3m_2}+\frac{125}{12}m_2\frac{(\mathbf{p}_1\cdot\mathbf{p}_2)(\mathbf{n}_{12}\cdot\mathbf{p}_1)(\mathbf{n}_{12}\cdot\mathbf{p}_2)}{m_1^2m_2^2}+\frac{10}{3}m_2\frac{(\mathbf{n}_{12}\cdot\mathbf{p}_1)^2(\mathbf{n}_{12}\cdot\mathbf{p}_2)^2}{m_1^2m_2^2}$$
$$\left.-\frac{1}{48}(220m_1+193m_2)\frac{\mathbf{p}_1^2(\mathbf{n}_{12}\cdot\mathbf{p}_2)^2}{m_1^2m_2^2}\right]+\frac{G^3m_1m_2}{r_{12}^3}\left[-\frac{1}{48}\left(466m_1^2+\left(473-\frac{3}{4}\pi^2\right)m_1m_2+150m_2^2\right)\frac{\mathbf{p}_1^2}{m_1^2}\right.$$
$$+\frac{1}{16}\left(77(m_1^2+m_2^2)+\left(143-\frac{1}{4}\pi^2\right)m_1m_2\right)\frac{(\mathbf{p}_1\cdot\mathbf{p}_2)}{m_1m_2}+\frac{1}{16}\left(61m_1^2-\left(43+\frac{3}{4}\pi^2\right)m_1m_2\right)\frac{(\mathbf{n}_{12}\cdot\mathbf{p}_1)^2}{m_1^2}$$
$$\left.+\frac{1}{16}\left(21(m_1^2+m_2^2)+\left(119+\frac{3}{4}\pi^2\right)m_1m_2\right)\frac{(\mathbf{n}_{12}\cdot\mathbf{p}_1)(\mathbf{n}_{12}\cdot\mathbf{p}_2)}{m_1m_2}\right]$$
$$+\frac{1}{8}\frac{G^4m_1m_2^3}{r_{12}^4}\left[\left(\frac{227}{3}-\frac{21}{4}\pi^2\right)m_1+m_2\right]+(1\longleftrightarrow 2). \tag{12}$$

3 PN (~3 LOOP) MULTIPOLE MOMENTS OF BINARY BLACK HOLE

- REPLACE

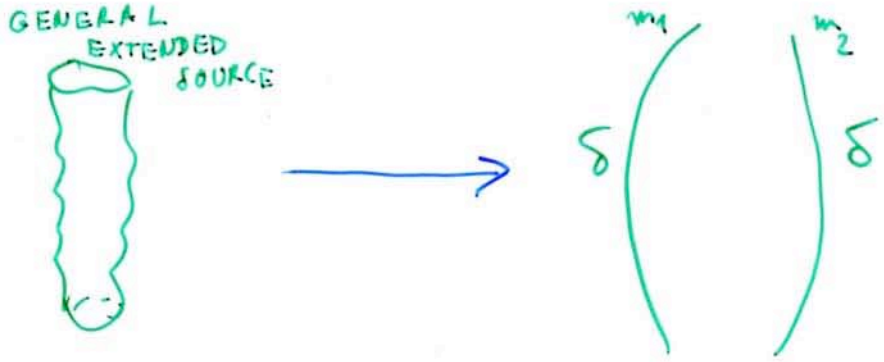

- MULTIPOLE MOMENTS:

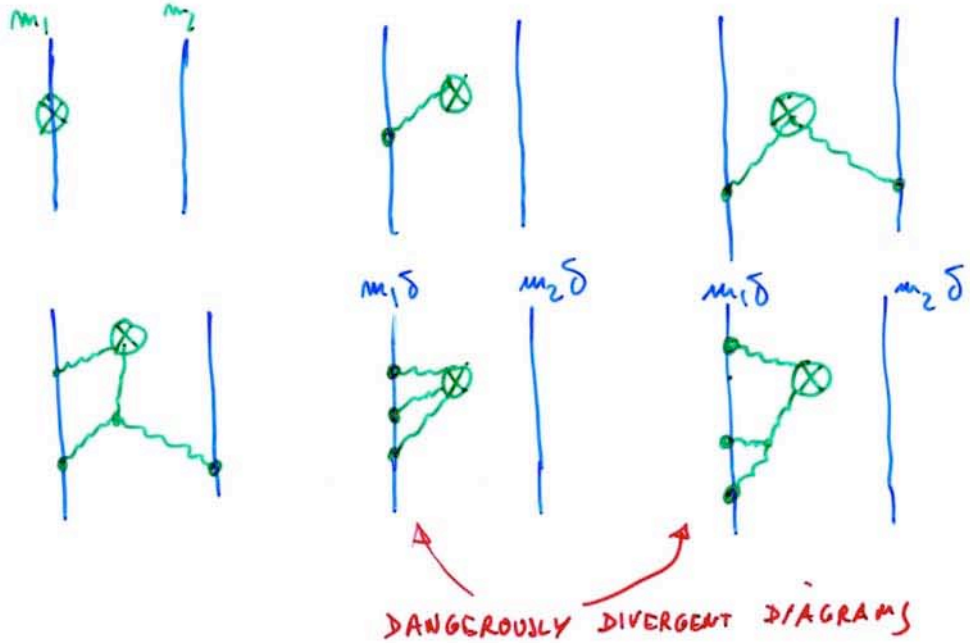

- NEED DIMENSIONAL REGULARIZATION TO COMPLETE THE CALCULATION
(Blanchet, Damour, Esposito-Farèse, Iyer '05)

Nice 4.9
ST THOMAS 9

"TAYLOR" PN-EXPANDED RESULTS :

RADIATION FROM BINARY SYSTEM

Blanchet et al...

$\gamma \equiv \frac{GM}{r_{harmonic}}$ $\quad \nu = m_1 m_2 / M^2$

- $\frac{I_{ij}}{\nu} = \left(1 + \gamma\left(-\frac{1}{42} - \frac{13}{4}\nu\right) + \gamma^2\left(-\frac{461}{152} - \frac{18395}{1512}\nu \dots\right) + \gamma^3\left(\dots + \dots\nu + \dots\nu^2 + \nu^3 + \ln\right)\right)\hat{x}^{ij}$ $+ \dots$

- $U_{ij} = I_{ij}^{(2)} + \text{TAILS} + \cdots$

- $\frac{dE}{dt} = \frac{1}{5}\left(U_{ij}^{(1)}\right)^2 + \cdots\left(U_{ijk}^{(2)}\right)^2 + \cdots\left(V_{ij}^{(1)}\right)^2 + \dots$

- $\frac{dE}{dt} = \frac{32}{5}\frac{c^5}{G}\nu^2 \gamma^5 \left\{1 + \left(-\frac{2927}{336} - \frac{5}{4}\nu\right)\gamma + \left(\dots + \dots\nu\right)\gamma^2 + \left(\dots + \dots\nu + \dots\nu^2 + \ln\right)\gamma^3\right\}$

$\gamma = \frac{GM}{c^2 r}$ harmonic coords

IN TERMS OF $\quad \boxed{v_\omega \equiv \left(\frac{GM\omega}{c^3}\right)^{1/3}}$

- $\frac{dE}{dt} = \frac{32}{5}\nu^2 v_\omega^{10}\left\{1 + \left(-\frac{1247}{336} - \frac{35}{12}\nu\right)v_\omega^2 + 4\pi v_\omega^3 + \left(-\frac{44711}{9072} + \frac{9271}{504}\nu + \dots\right)v_\omega^4\right.$
$\left. + \left(\dots + \dots\nu\right)v_\omega^5 + \left(\dots + \dots\nu + \dots\nu^2\right)v_\omega^6 + \left(\dots + \dots\nu\right)v_\omega^7\right.$

ALL KNOWN FOR $\nu \neq 0$

$+ A_8^0 v_\omega^8 + A_9^0 v_\omega^9 + A_{10}^0 v_\omega^{10} + A_{11}^0 v_\omega^{11}$

KNOWN ONLY FOR $\nu = 0$: TEST-MASS LIMIT

Poisson ; Tanaka Tagoshi Sasaki '96

RESUMMATION TECHNIQUES

EG. GW ENERGY FLUX AT THE LSO (FOR TEST PARTICLE)

IN HARMONIC COORDS $\gamma = \frac{GM}{c^2 r_h}$

$$F_{TM}(\gamma) = 1 - 1.74(5\gamma) + 1.12(5\gamma)^{3/2} + 1.29(5\gamma)^2 + \dots$$

($=1$ AT SCHWARZ. LSO "$R = 6GM$", $r_h = 5GM$)

NO CONVERGENCE AT ALL

INVARIANT FUNCTION $F(x)$ $\quad x \equiv \left(\frac{GM\omega^{orb}}{c^3}\right)^{2/3}$ IN SCHW: $x = \frac{GM}{c^2 R} = \frac{1}{6}$ AT LSO

$$F_{TM}(x) = 1 - 0.619(6x) + 0.855(6x)^{3/2} - 0.137(6x)^2 + \dots$$

SLOW CONVERGENCE

BUT CONVERGENCE BECAUSE

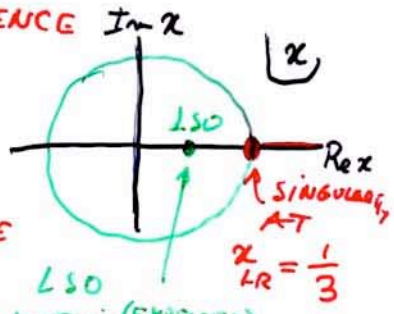

NEED AN ACCELERATOR OF CONVERGENCE

USE PN INFORMATION IN OPTIMAL WAY

TECHNIQUES

(ALL DETERMINED AT 3PN DJSbg)

- WORK ONLY WITH INVARIANT FUNCTIONS
- USE KNOWLEDGE OF TEST-MASS LIMIT, TAKING $\nu \equiv \frac{m_1 m_2}{(m_1+m_2)^2}$ AS DEFORMATION PARAMETER (NOT ASSUMED SMALL)
- INTRODUCE NEW FUNCTIONS
- USE PADÉ RESUMMATION

Nice 4.12

TAYLOR APPROXIMANTS TO $\dot{E}/\dot{E}_N$

Damour Iyer Sathyaprakash '98

$\nu=0$ TEST-MASS

Exact Numerical from Poisson

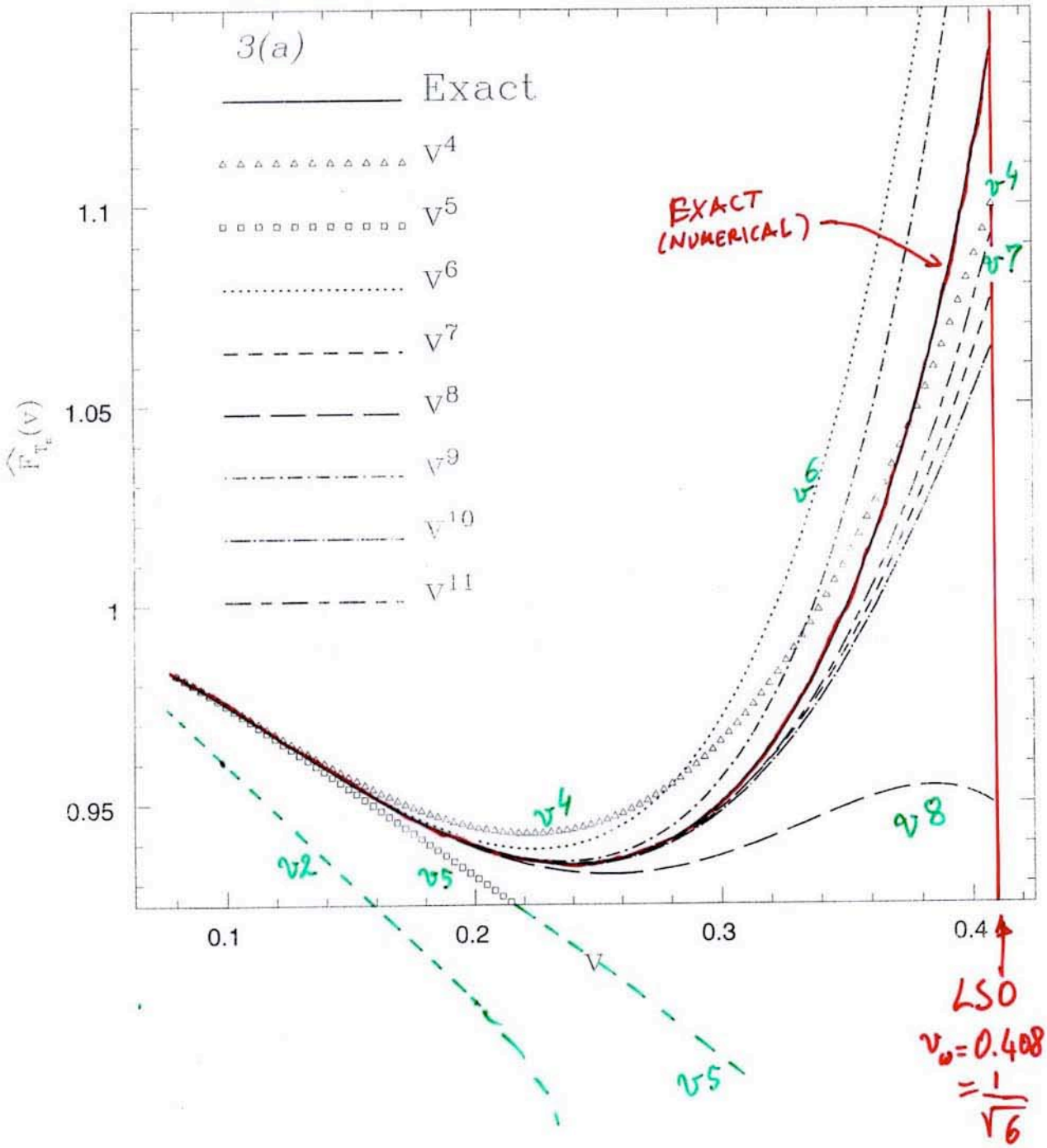

Mia 4.13

PADÉ APPROXIMANTS TO $\dot{E}/\dot{E}_N$

$\nu = 0$ TEST-MASS

Damour Iyer Sathyaprakash '98
Exact Numerical from Poisson

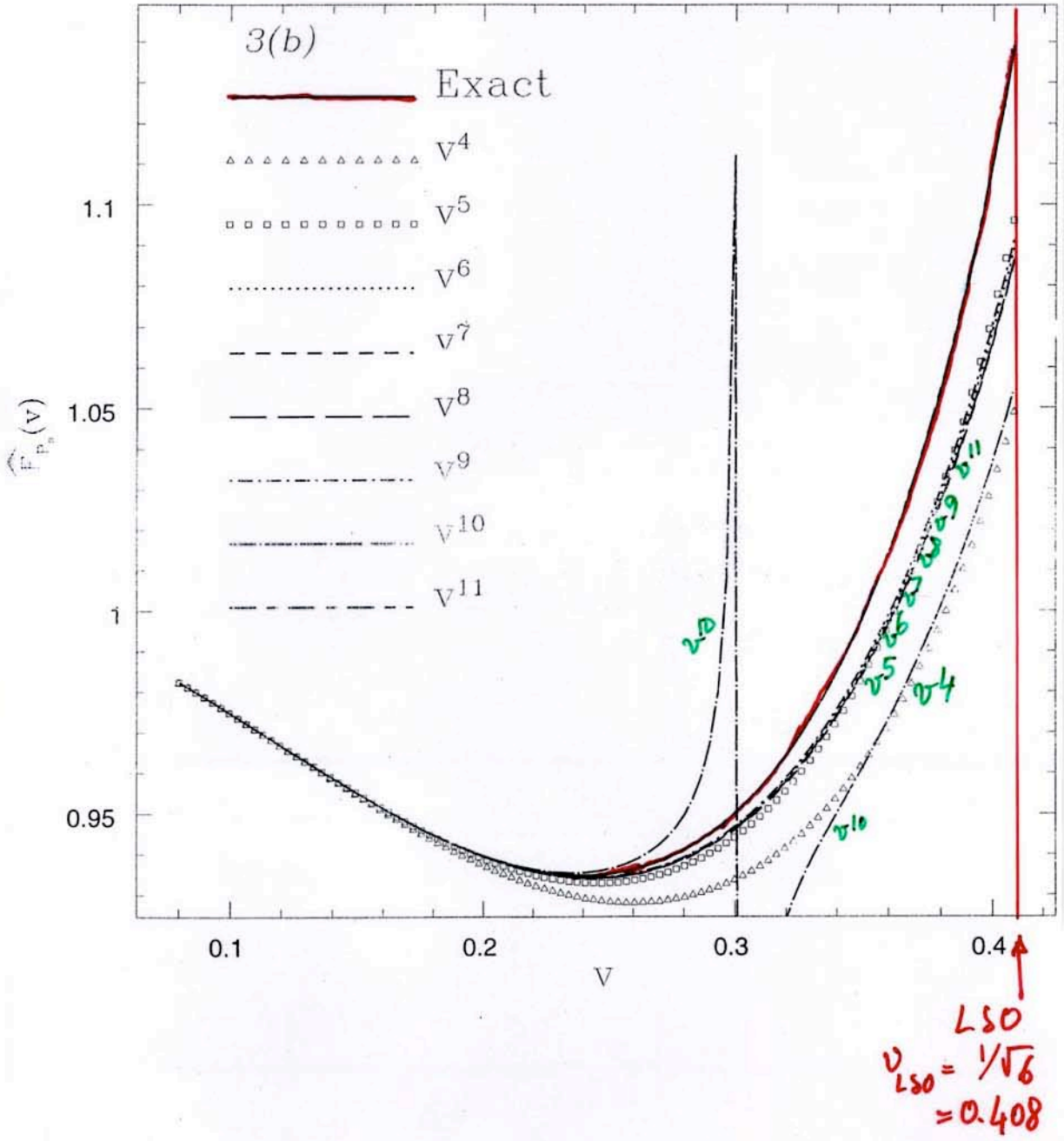

RESULTS AT 2.5 PN

RESUMMED RADIATION REACTION FOR CIRCULAR ORBITS

LET $\boxed{v \equiv \left(\frac{GM\omega}{c^3}\right)^{\frac{1}{3}} \equiv x^{1/2}}$

ANG. MOMENTUM RR: $\mathcal{F}_\varphi^{PN} = -\frac{32}{5G}\nu^2 \frac{v^{10}}{\omega}\left[1 + a_2 v^2 + a_3 v^3 + a_4 v^4 + a_5 v^5\right]$

$a_2 = 1$

COEFFICIENTS DEPEND ON ν

INVARIANT FUNCTION BUT BAD BECAUSE $\exists$ NO $a_1 v^1$

eg. $a_2(\nu) = -\frac{1247}{336} - \frac{35}{12}\nu$

$\Rightarrow$ INJECT INFO THAT $\mathcal{F}_\varphi^{TM}$ HAS A SIMPLE POLE AT $v = v_{LR}^{TM} \simeq \frac{1}{\sqrt{3}}$

$\Rightarrow$ NEW FUNCTION: $\hat{\mathcal{F}} = \left(1 - \frac{v}{v_{pole}(\nu)}\right) \times \mathcal{F} = \cdots\left[1 + v + v^2 + \cdots\right]$

PADÉ THIS EXPANSION

$$\mathcal{F}_\varphi\left(\omega = \frac{d\varphi}{dt}\right) = -\frac{32}{5G}\nu^2 \frac{v^{10}}{\omega} \frac{1}{1 - \frac{v}{v_{pole}(\nu)}} \cfrac{1}{1 + \cfrac{c_1(\nu)v}{1 + \cfrac{c_2(\nu)v}{1 + \cfrac{c_3(\nu)v}{1 + \cfrac{c_4(\nu)v}{1 + c_5(\nu)v}}}}}$$

Damour, Iyer, Sathyaprakash '98

$\nu = \frac{1}{4}$ TAYLOR $\widehat{\text{FLUX}}$

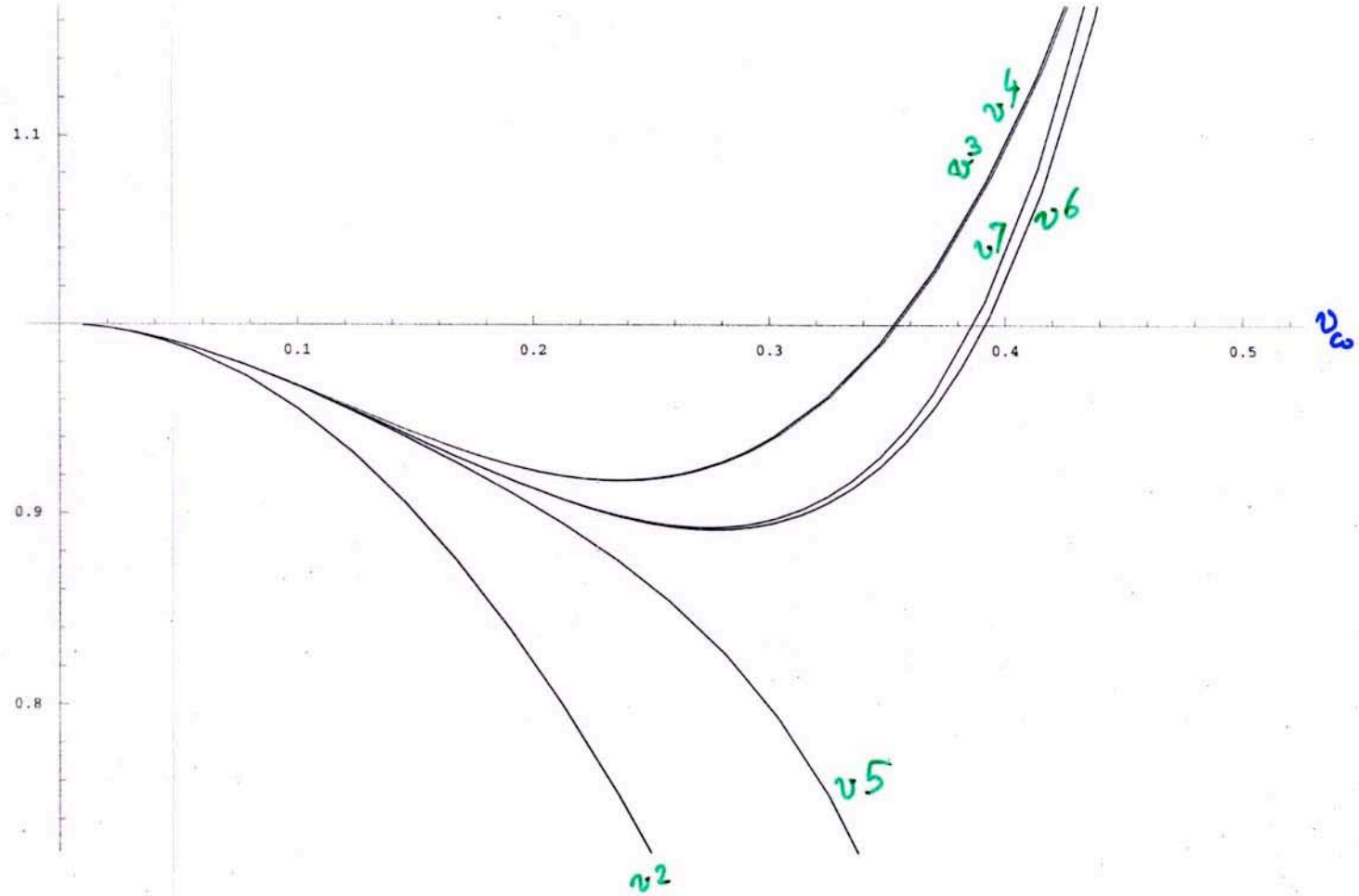

$\nu = \frac{1}{4}$ PADÉ FLUX

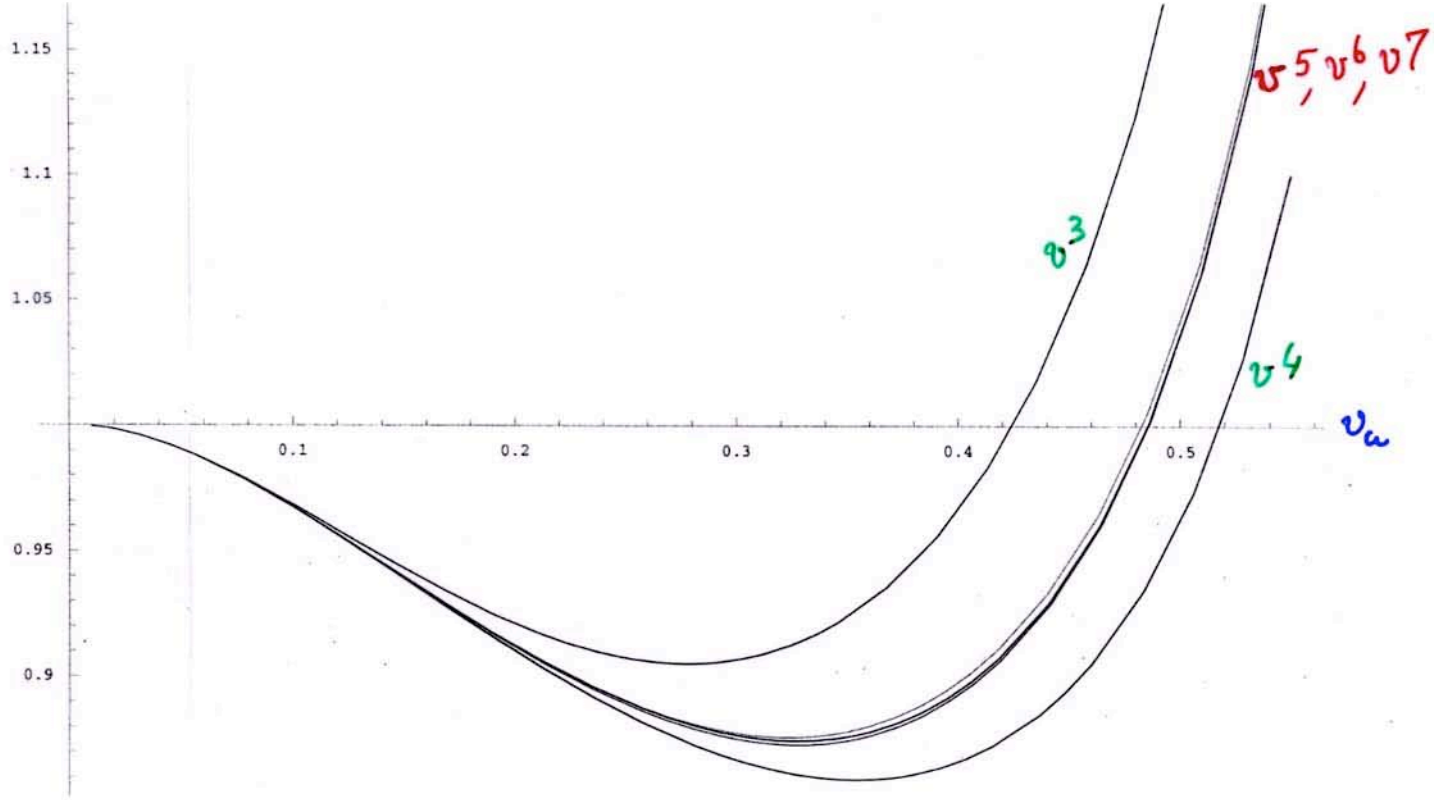

$\nu = 1/4$ TAYLOR $\widehat{\text{FLUX}} \times (1 - v/v_{\text{pole}(v)})$

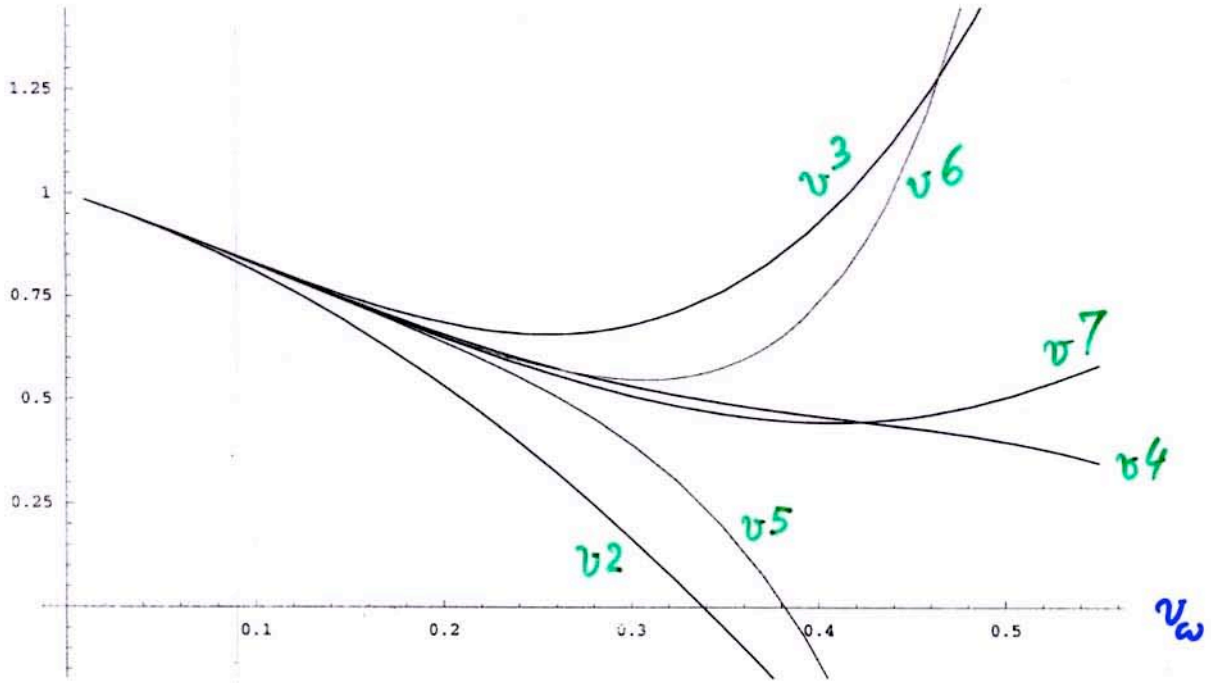

$v = 1/4$ PADÉ $\hat{F}LUX \times (1 - v/v_{pole}(v))$

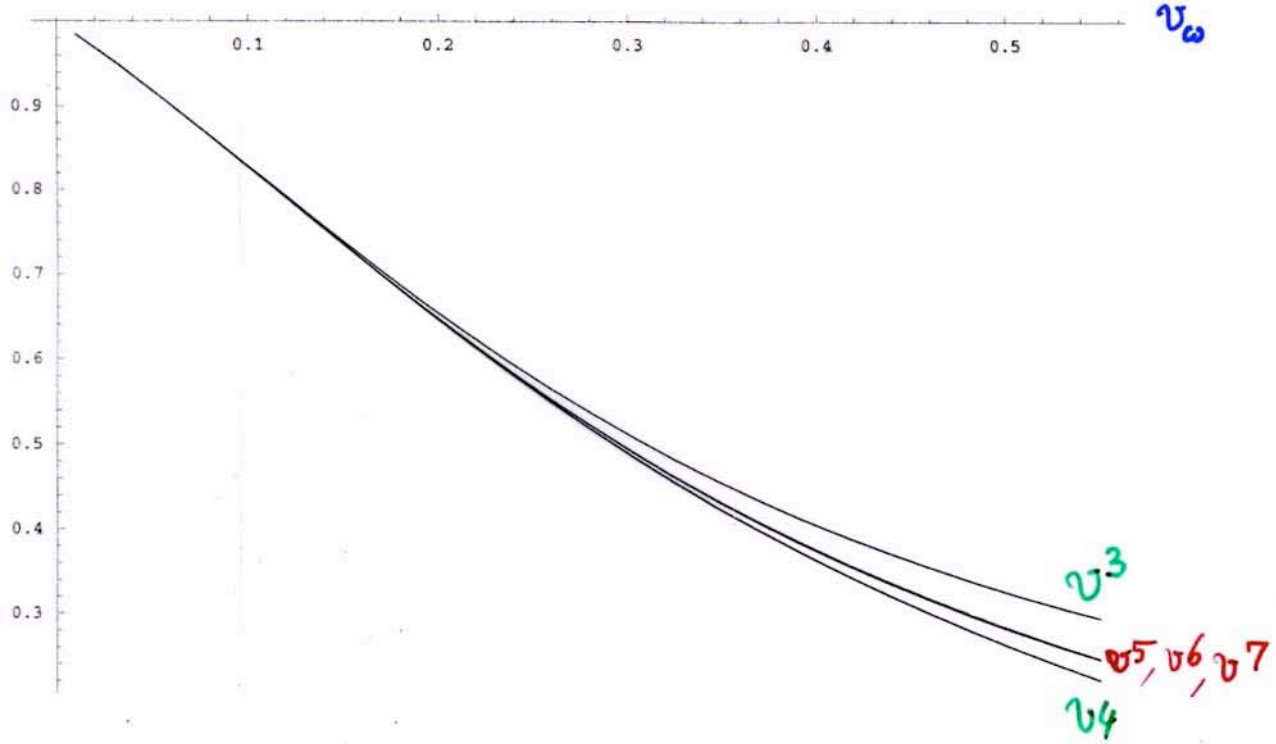

Nice 4.14

RESUMMATION OF THE (CONSERVATIVE) DYNAMICS

- SEVERAL POSSIBILITIES EXPLORED & COMPARED (DIS 98, DJS 00)
- MOST ROBUST, EFFICIENT AND VERSATILE (AND ELEGANT!)

"EFFECTIVE ONE-BODY" APPROACH

BASIC IDEA STARTED IN QED (Brézin Itzykson Zinn-Justin 70; Todorov 70)

NEW FORM ADAPTED TO GR (Buonanno Damour 99, 00; Damour 01; Damour Jaranowski Schäfer 00)

QUANTUM ENERGY STATES OF TWO DIFFERENT SYSTEMS

REAL SYSTEM IN THE CENTER OF MASS FRAME

EFFECTIVE SYSTEM

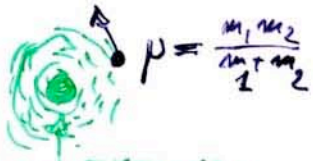

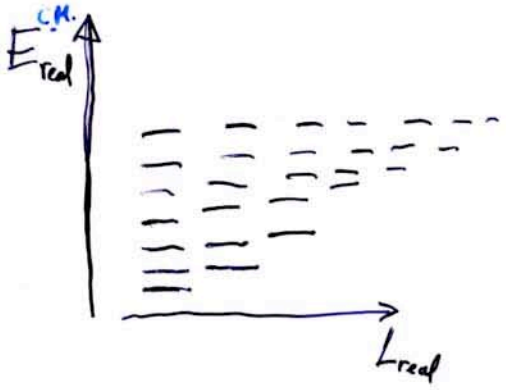

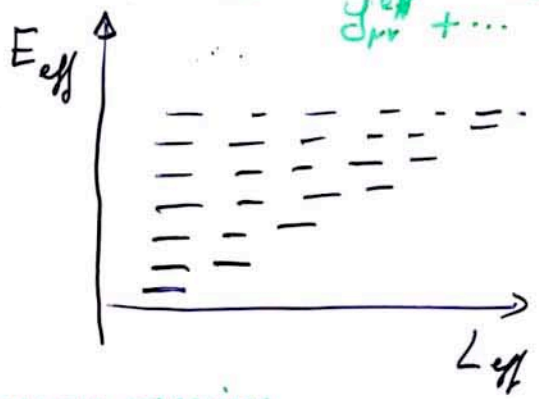

i.e. DELAUNAY HAMILTONIAN

ADIABATIC INVARIANTS $I_i = \oint p_i \, dq^i$

$$E^{C.M.}_{real} = E_{real}(L_{real}, N_{real}) \qquad E_{eff} = E_{eff}(L_{eff}, N_{eff})$$

MAPPING:

$$\begin{cases} L_{real} = L_{eff} \\ N_{real} = N_{eff} \\ E_{real} = f(E_{eff}) \end{cases}$$

BEING $L_{eff}/\hbar,\ L_{real}/\hbar,\ N_{real}/\hbar,\ N_{eff}/\hbar \in \mathbb{N}$

DETERMINES f AND $g^{eff}_{\mu\nu}(x^\mu) + \dots$

Nice 4.15

EOB: ENORMOUS SIMPLIFICATION OF DYNAMICS

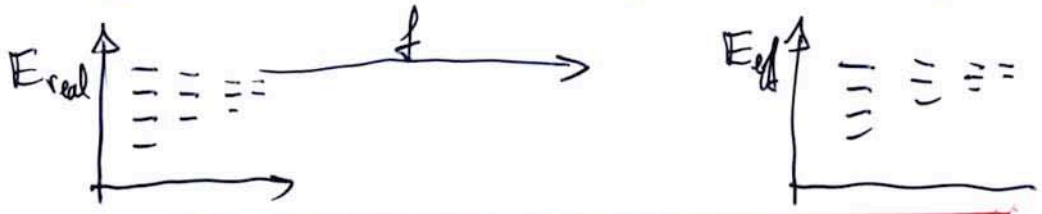

f ALWAYS UNIVERSAL:

$$\frac{E_{eff}}{\mu} = \frac{E_{real}^2 - m_1^2 - m_2^2}{2 m_1 m_2}$$

$$\left[+ \left|_{real}^{CM} \right]^{2PN} = \frac{1}{2\mu}\vec{p}^2 - \frac{GM}{r} + \frac{1}{c^2}\left(p^4 + \dots \frac{(GM)^2}{r^2}\right) + \frac{1}{c^4}\left(p^6 + p^4\frac{GM}{r} + \dots + \left(\frac{GM}{r}\right)^3\right)$$

13 TERMS

NB: ~~1PN~~ 1PN CORRECTIONS!

$\Longleftrightarrow$ GEODESIC MOTION OF PARTICLE OF MASS μ IN

$$ds^2 = -A(r)dt^2 + \frac{D(r)}{A(r)}dr^2 + r^2 d\Omega^2$$

$$A^{2PN}(r) = 1 - \frac{2GM}{r} + 2\nu\left(\frac{GM}{r}\right)^3$$

$$D^{2PN}(r) = 1 - 6\nu\left(\frac{GM}{r}\right)^2$$

Buonanno Damour '00

@ 3PN NEED TO ADD p^4 TERMS TO GEODESIC H.J: $p^2 + p^2 + O(\vec{p}^4/c^0)$

2.4 TERMS IN C.M.

$$A^{3PN}(r) = 1 - \frac{2GM}{r} + 2\nu\left(\frac{GM}{r}\right)^3 + \left(\frac{94}{3} - \frac{41}{32}\pi^2\right)\nu\left(\frac{GM}{r}\right)^4$$

$$D^{3PN}(r) = 1 - 6\nu\left(\frac{GM}{r}\right)^2 + 2(3\nu - 26)\nu\left(\frac{GM}{r}\right)^3$$

Damour Jaranowski Schäfer 00

Nice 4.16

EFFECTIVE ONE BODY METRIC @ 2PN, 3PN

1PN

& ALWAYS : $\frac{E_{eff}}{\mu} = \frac{E_{real}^2 - m_1^2 - m_2^2}{2 m_1 m_2}$

1PN $H^{C.M.}_{1PN}$ = 6 TERMS → GEODESIC MOTION OF PARTICLE μ IN SCHWARZSCHILD:

(REDUCED TO C.M.)

$$ds^2_{EFF} = -\left(1 - \frac{2GM}{r}\right)dt^2 + \frac{dr^2}{1 - \frac{2GM}{r}} + r^2 d\Omega^2$$

2PN $H^{C.M.}_{2PN} = 6 + 7$ TERMS → GEODESIC MOTION ON

(condensed)

$$ds^2_{EFF} = -A(r)\,dt^2 + \frac{D(r)}{A(r)}dr^2 + r^2 d\Omega^2$$

$$\nu \equiv \frac{m_1 m_2}{(m_1+m_2)^2} \qquad 0 \le \nu \le 1/4$$

$$A^{2PN}(r) = 1 - \frac{2GM}{r} + 2\nu\left(\frac{GM}{r}\right)^3$$

$$D^{2PN}(r) = 1 - 6\nu\left(\frac{GM}{r}\right)^2$$

ν = DEFORMATION PARAMETER

3PN $H^{C.M.}_{3PN} = 6 + 7 + 11$ → condensed in 3 coefficients OF WHICH ONLY ONE IS REALLY IMPORTANT

$$A^{3PN}(r) = 1 - \frac{2GM}{r} + 2\nu\left(\frac{GM}{r}\right)^3 + \left(\frac{94}{3} - \frac{41}{32}\pi^2 + 2\omega_s\right)\nu\left(\frac{GM}{r}\right)^4$$

$$D^{3PN}(r) = 1 - 6\nu\left(\frac{GM}{r}\right)^2 + 2(3\nu - 26)\,\nu\left(\frac{GM}{r}\right)^3$$

$$+: \quad p^2 \to p^2\left[1 + 2(4-3\nu)\,\nu\left(\frac{GM}{r}\right)^2\left(\frac{\vec{n}\cdot\vec{p}}{\mu}\right)^4\right]$$

RADIAL FUNCTION

$$-g_{00}(r) \equiv A(r)$$

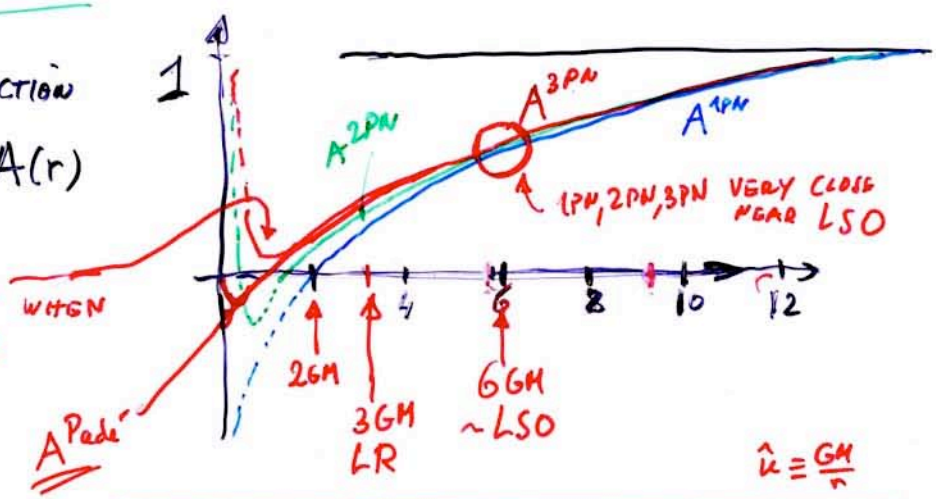

"UNPHYSICAL" WHEN $r \lesssim 2$

IMPROVED PADÉ ("RESUMMED")

$$\hat{u} \equiv \frac{GM}{r}$$

$$A(r) \equiv P^1_3\left[A^{3PN}(r)\right] = \frac{1 - a_1\hat{u}}{1 + b_1\hat{u} + b_2\hat{u}^2 + b_3\hat{u}^3}$$

+ RECENT INCLUSION OF SPIN EFFECTS (Damour 01)

Binding energy along a sequence (Damour, Gourgoulhon, Grandclément '02)

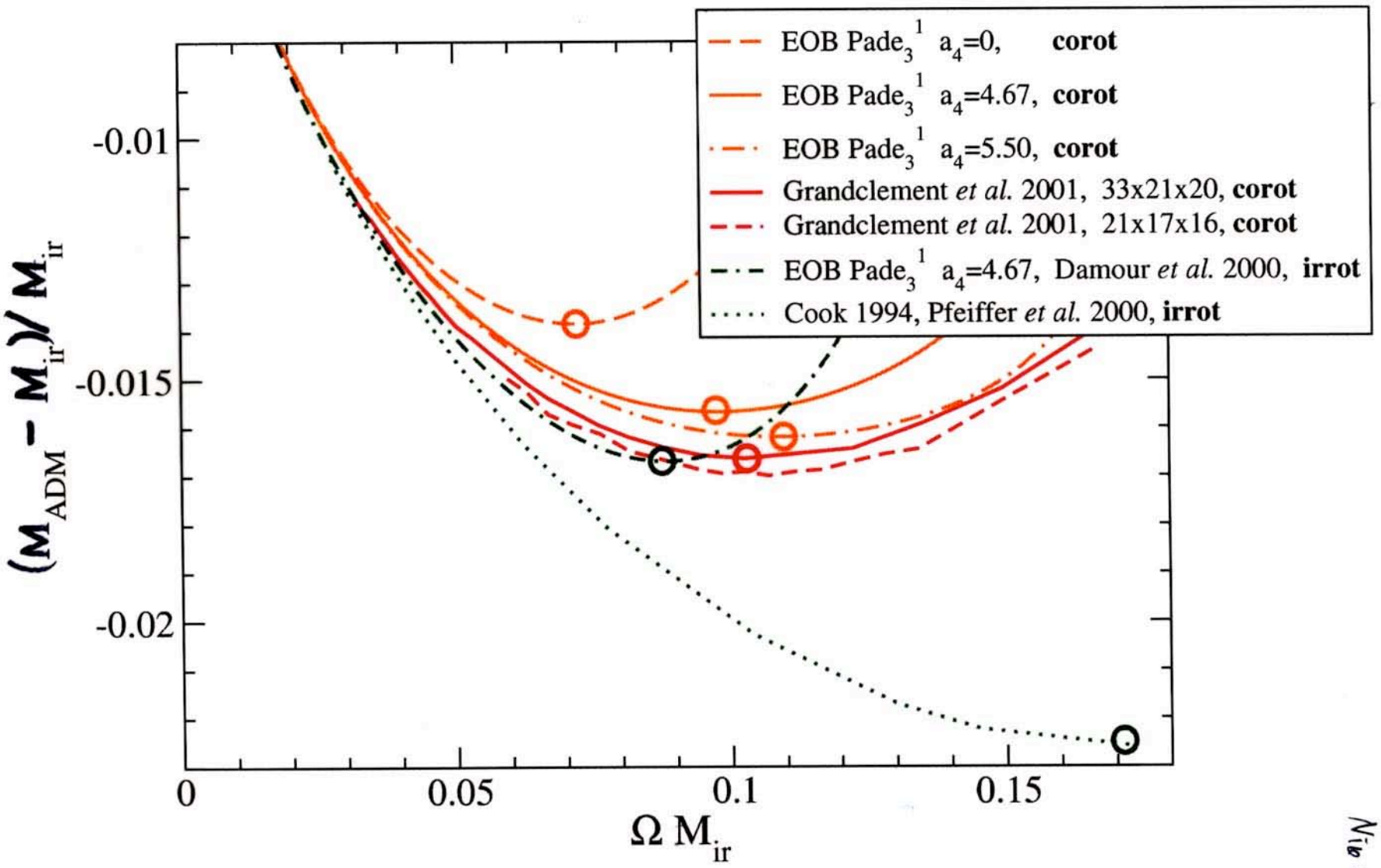

Nice 4.22

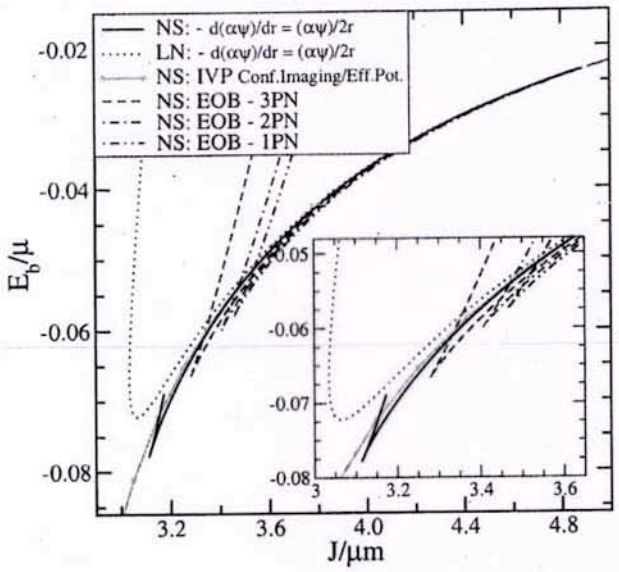

FIG. 11: Binding energy vs. total angular momentum along the sequence of *non-spinning* (NS) equal-mass black holes (as defined by the Komar-mass condition). For comparison, the leading-order non-spinning (LN) results from our earlier work [5] are included, as well as results from Refs. [9, 10].

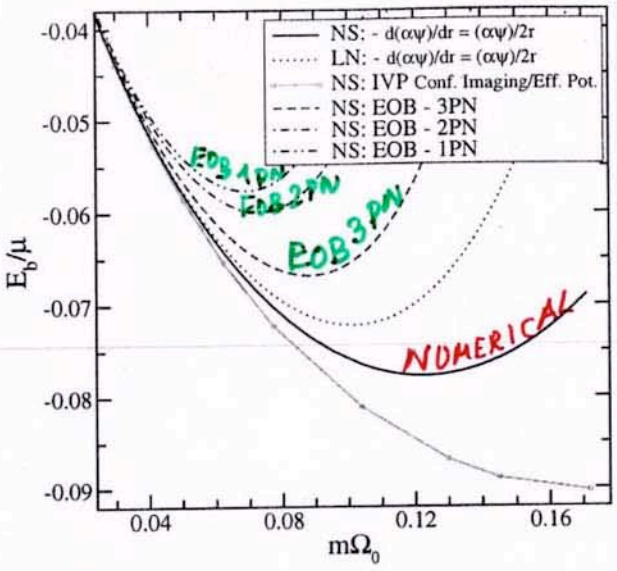

FIG. 12: Binding energy vs. orbital frequency along the sequence of *non-spinning* (NS) equal-mass black holes (as defined by the Komar-mass condition). Lines are labeled as in Fig. 11.

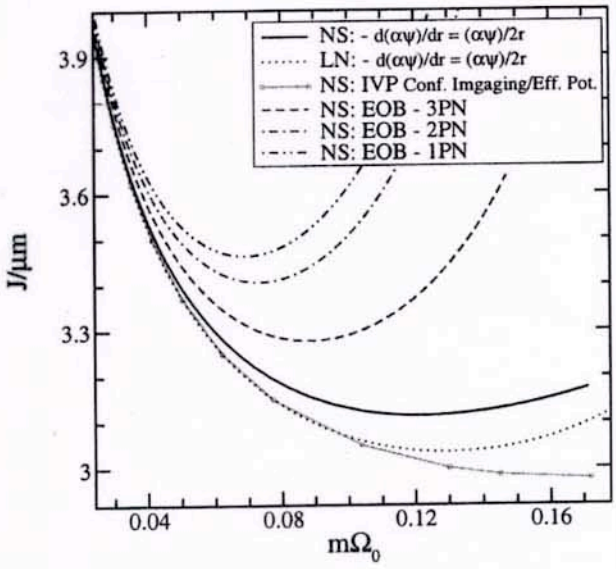

FIG. 13: Total angular momentum vs. orbital frequency along the sequence of *non-spinning* (NS) equal-mass black holes (as defined by the Komar-mass condition). Lines are labeled as in Fig. 11.

earlier initial-data method[9], and to the results based on the leading-order method of defining non-spinning black holes. While the difference between our improved numerical results and those based on the leading-order method are not dramatic, they do become significant at small separations.

The most remarkable change produced by the improved method is seen in Fig. 11 which plots the dimensionless binding energy as a function of the dimensionless total angular momentum. Using the leading-order method, the sequence did not approximate a cusp at the ISCO as we would have expected. However the improved data clearly approximates a cusp. In Ref.[5], we pointed out that we did not understand why our non-spinning data lacked this feature. We now understand that the approximate cusp is a necessary feature of a sequence that is in good agreement with the EP method. This can be seen by looking at Figs. 6 and 8 and considering the behavior near the inflection point of Fig. 8 that defines the ISCO for the EP method. In fact, a sequence of circular orbits defined by the EP method necessarily has the minima in E_b/μ and $J/\mu m$ coincide, resulting in an exact cusp in the sequence at ISCO.

We can also reexamine how well the improved non-spinning data agrees with the thermodynamic identity of Eq. (41). The third column of Table I shows $M_{\rm irr}$ along a sequence of non-spinning equal-mass binaries in circular orbit constructed using the Komar-mass condition. Comparing to the results of the second column for the corresponding case of corotation, we see that the new approach for defining non-spinning binaries yields results that are comparable in magnitude. Also, the variation in $M_{\rm irr}$ is much smaller than those seen in leading-order non-spinning data of the last column.

Finally, it is interesting to reconsider the sequence of non-spinning circular orbits constructed by the EP method. Recalling that an exact stationary solution of

EOB APPROACH

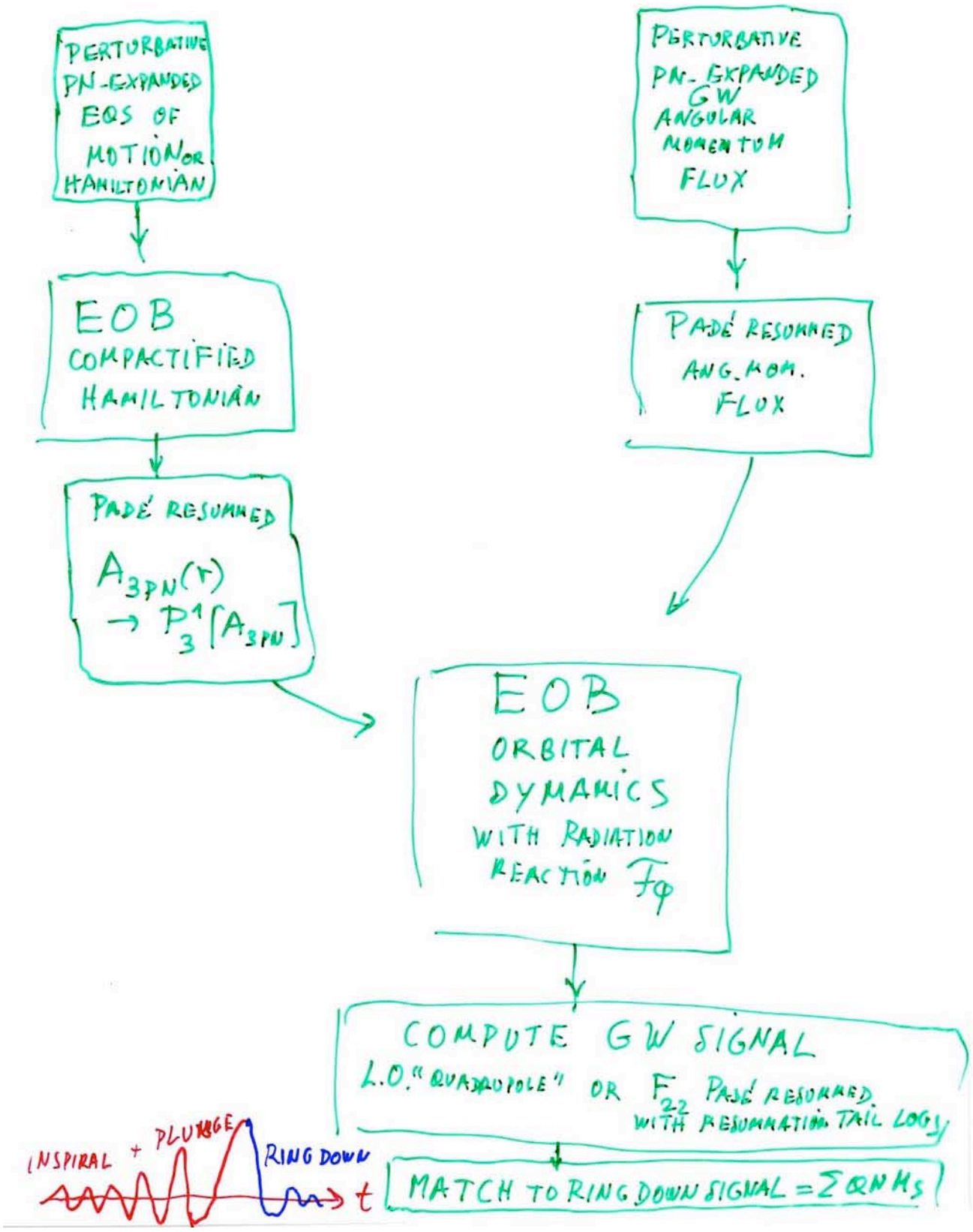

Nice 4.24

INSPIRAL, PLUNGE AND MERGER VIA EOB FORMALISM

Buonanno Damour 00

- EQS OF MOTION (QUASI-CIRCULAR ORBITS)

$$\begin{cases} \dfrac{dr}{dt} = \dfrac{\partial \mathcal{H}(r, P_r, P_\varphi)}{\partial P_r} \\ \dfrac{d\varphi}{dt} \equiv \omega = \dfrac{\partial \mathcal{H}(r, P_r, P_\varphi)}{\partial P_\varphi} \\ \dfrac{dP_r}{dt} = -\dfrac{\partial \mathcal{H}(r, P_r, P_\varphi)}{\partial r} \\ \dfrac{dP_\varphi}{dt} = \mathcal{F}_\varphi \end{cases}$$

EOB (RESUMMED) HAMILTONIAN

$$\mathcal{H} = \frac{1}{\nu}\sqrt{1 + 2\nu\left[\sqrt{A(r)\left(1 + P_r^2 + \frac{P_\varphi^2}{r^2} + \frac{A(r)}{B(r)} P_r^2 + O(\nu^4)\right)} - 1\right]}$$

EFFECTIVE METRIC COEFF

PADÉ-RESUMMED RADIATION REACTION = ANG. MOM. LOSS

$$\mathcal{F}_\varphi = -\frac{32}{5}\eta\,\omega^5 (r^2)^4 \quad \begin{matrix} \uparrow \text{Padé} \\ \uparrow \text{DIS} \end{matrix} \; \underline{(\omega r^2)^{4/3}, \nu)}$$

$$1 - \omega r^2 P^{1/3}/\gamma_{\text{pole}}$$

- USE SOME $h_{ij}^{TT} = \mathcal{F}[\vec{x}, \vec{v}]$ TO ESTIMATE GW SIGNAL
- AFTER CROSSING $r = 3$ (LIGHT RING)

→ MATCH TO RING-DOWN GW SIGNAL MADE OF QUASI-NORMAL MODES

(cf Davis Ruffini Press Price 1971)

(RESUMMED) EFFECTIVE ONE BODY DYNAMICS + RESUMMED RADIATION REACTION (QUASI-CIRCULAR ORBITS)

NI6 4.247 T815b

TRANSITION INSPIRAL → PLUNGE WITH ARBITRARY MASS RATIO

① YIELDS INITIAL DYNAMICAL DATA $(q_1 q_2 P_1 P_2)$ AT BEGINNING OF PLUNGE: 0.6 ORBIT LEFT

GOOD IN VIEW OF STATE OF THE ART NUMERICAL SIMULATIONS (Pretorius 05)

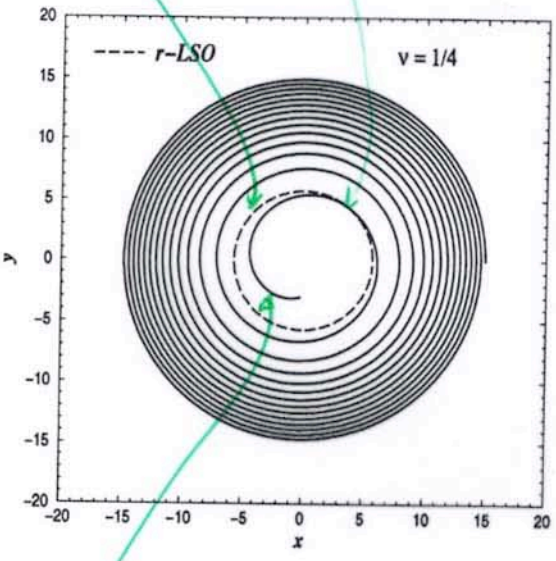

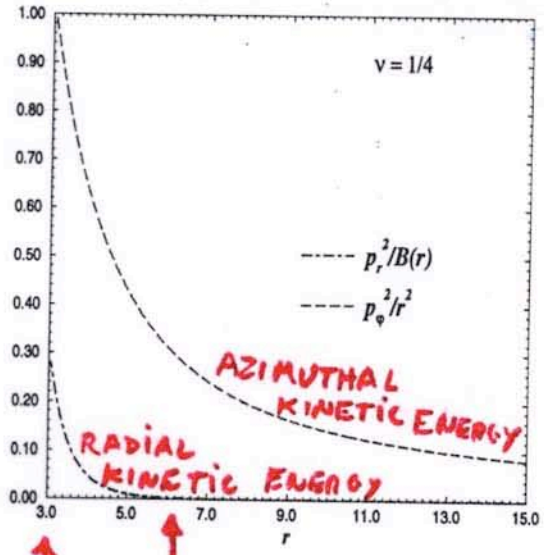

LIGHT-RING

LSO

REMAINS QUASI-CIRCULAR DURING THE WHOLE PLUNGE

② FIRST ESTIMATE OF FULL WAVEFORM: "6M" → "3M" ≃ MERGER

Nov 4.27

WAVEFORM FROM PRECESSING BINARIES OF SPINNING BLACK HOLES, USING EOB

Buonanno Chen Damour

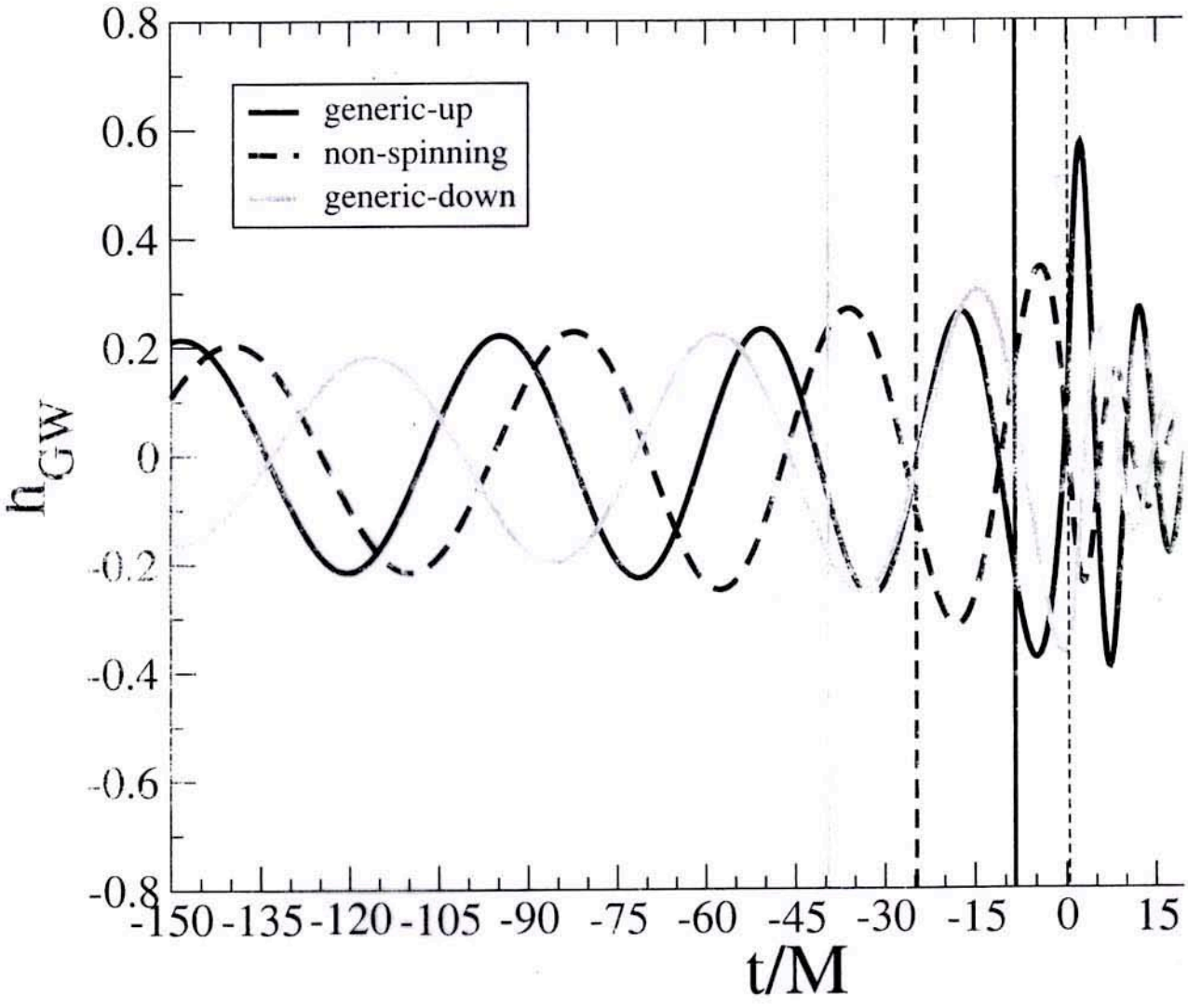

EOB 'PREDICTIONS'

- QUALITATIVELY

COMPARISON WITH NUMERICAL RESULTS

- ∃ BLURRED TRANSITION FROM INSPIRAL TO PLUNGE ✓ Pretorius '06, Baker et al '06, Campanelli, Lousto, Marronetti, Z., Campanelli, '06
- 'PLUNGE' IS A CONTINUATION OF INSPIRAL WITH $\mathcal{N} \simeq (4\nu)^{-\frac{1}{5}}$ EXTRA ORBITS ✓ Lousto, Zlochower a
- TRANSITION PLUNGE → RINGDOWN IS VERY FAST, AND CAN BE MODELLED BY QNM MATCHING AT END OF PLUNGE ✓
- FOR SPINNING BLACK HOLES (TD'01)

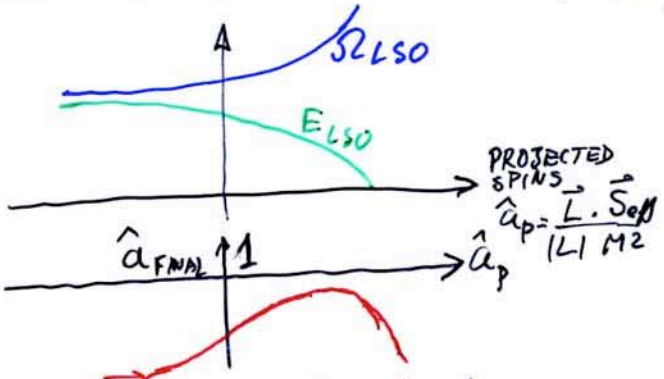

✓ Campanelli, Lousto, Zlochover

- FOR $\vec{P}$ LOSS AND RECOIL (TD, Gopakumar '06)

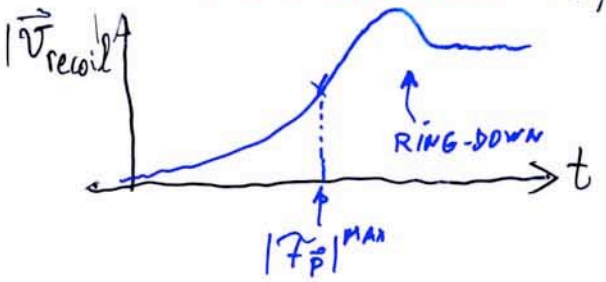

✓ Baker et al. '06 b

✓ Gonzalez et al '06

$$|\vec{v}_{RECOIL}| \propto \nu^2\sqrt{1-4\nu}\left\{1.1 - 1.\nu + 3\nu^2\right\}$$

↑ Fitchett 83 ↑ EOB

$$v_{rec} \propto \nu^2\sqrt{1-4\nu}\left\{1 - 0.93\nu\right\}$$

COMPARING QUANTITATIVE PREDICTIONS

- SPIN PARAMETER: $\hat{a} \equiv \frac{J}{M^2} = \frac{a_{Kerr}}{M}$

  OF FINAL BLACK HOLE (NO INITIAL SPINS)
  EQUAL MASSES

EOB 2PN
NEGLECTING RING-DOWN
(Buonanno, Damour '00a)

$\hat{a} \simeq 0.795$

WITH RING-DOWN
(Buonanno, Damour '00b)

$\hat{a} \simeq 0.795 - 5.35 \times 0.007$
$\simeq 0.757$ *

EOB 3 PN
NEGLECTING RING-DOWN
(Buonanno, Chen, Damour '06)

$\hat{a} \simeq 0.77$

NUMERICAL RESULTS
Pretorius, Baker et al.; Campanelli et al.

$\hat{a} \simeq 0.69$

EOB 3 PN
WITH SCALED SMALL ν RINGDOWN
(Damour, Nagar '06)

$\hat{a} \simeq 0.69$

NICE AGREEMENT

- CONSIDER $\hat{a}\left(\nu; \frac{S_1}{m_1^2}, \frac{S_2}{m_2^2}\right)$

COMPARING WAVEFORMS

- COMPARABLE-MASS CASE : $\nu = \frac{1}{4}$
  (Buonanno, Cook, Pretorius, '06) ; (Damour, Nagar, et al. '06)

- SMALL MASS-RATIO CASE : $\nu \ll 1$; SAY $\nu = 0.01$
  (Damour, Nagar '06) ; (Nagar, Damour, Tartaglia '06)
  USEFUL FRAMEWORK FOR COMPARING

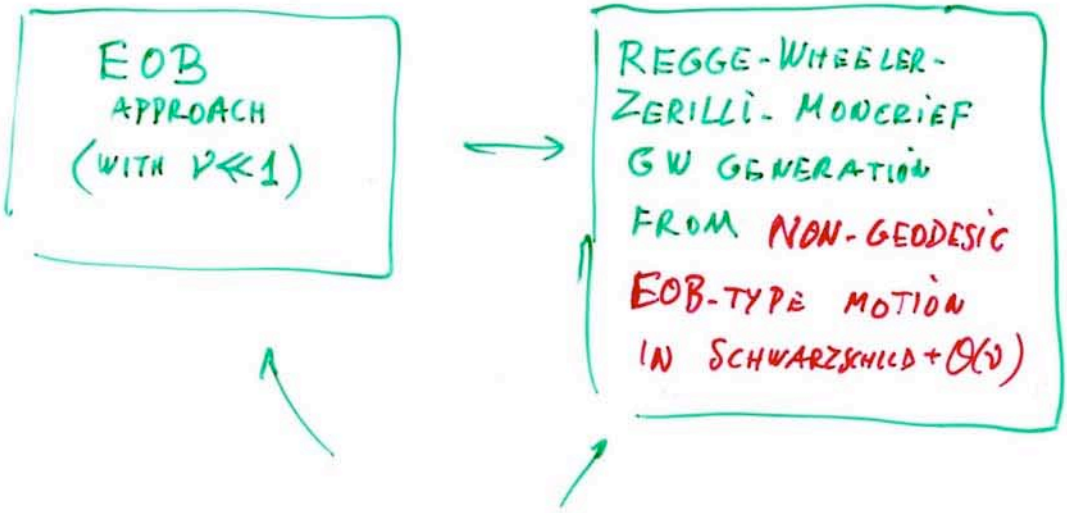

COMPARE GW WAVEFORMS

(Buonanno, Cook, Pretorius '06)

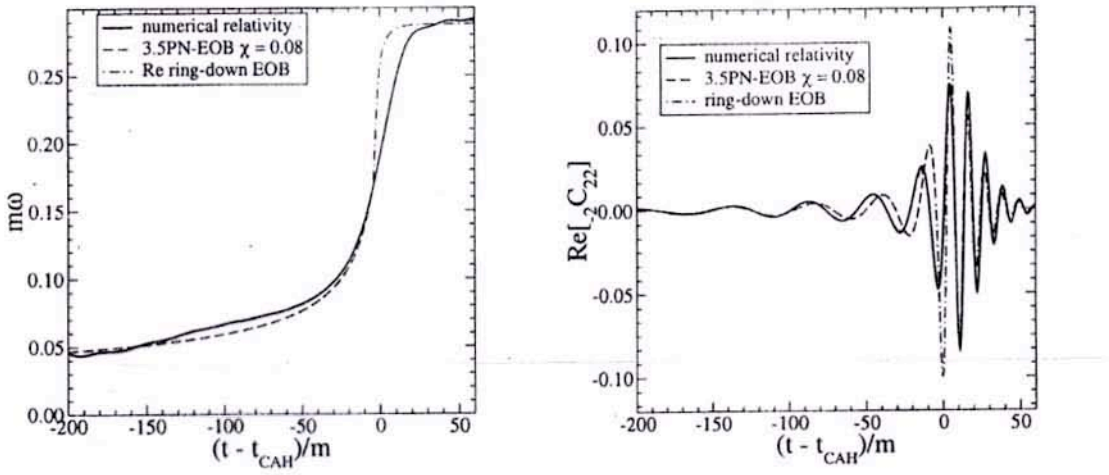

FIG. 21: We compare the NR and EOB frequency and $\mathrm{Re}[_{-2}C_{22}]$ throughout the entire evolution inspiral–merger–ring-down. The data refers to the $d = 16$ run.

By assuming the merger is a very short phase, the authors of Ref. [28] simply joined the GW signal at the end of the inspiral to the least-damped QNM. As said above this modeling was inspired by the idea that once around the light-ring (i.e., inside the potential barrier), the GW emission is quickly dominated by the excitation of the QNM of the newly-formed BH. The choice of matching only one QNM inevitably creates a sudden jump of the GW frequency at the matching point. However, a smoother transition can be obtained by including higher overtones. As discussed in Sec. VI, the analysis done in Sec. V would suggest that the QNM production starts a bit later, around the peak of the radiation. At this stage we do not know whether a linear superposition of QNM can be responsible for raising the frequency from around the light ring (see Fig. 18) to the peak of radiation. Following an effective approach aimed at modeling the GW signal for detection, we push this idea further by including higher overtones when matching to the ring-down phase and discuss the consequences. The inclusion of higher overtones when matching to the ring-downn phase has also recently been adopted in Ref. [84], where the authors computed the transition inspiral–plunge–ring-down of a test particle in Schwarzschild. By including higher overtones, the authors could successfully match the exact numerical rise of frequency from the light ring to the least damped QNM as obtained from the Zerilli equation.

First, we evaluate the BH mass and angular-momentum at the end of the EOB plunge, finding $m_{\rm end} \equiv E_{\rm end} \simeq 0.971\,m$ and $a_{\rm end}/m_{\rm end} \equiv J_{\rm end}/E^2_{\rm end} \simeq 0.785$. Then, we notice that those values *are not* the final BH mass and angular momentum because the binary has yet to emit energy and angular-momentum from the light-ring or CAH to the least-damped mode (see discussions around Fig. 18). Future NR simulations will provide predictions for different mass ratios and spins. Here, guided by the results of Sec. VI and Fig. 18, we assume that $(m_{\rm end} - M_f)/m_{\rm end} = 1.5\%$ and $(a_{\rm end} - a_f)/a_{\rm end} = 6\%$. Thus, we obtain $M_f = 0.956\,m$ and $a_f/M_f = 0.738$. Using Ref. [75], we determine the frequency and the decay time of the fundamental mode and the first two overtones, finding $m\omega_{220} = 0.576$, $m\omega_{221} = 0.565$, $m\omega_{222} = 0.545$, $\tau_{220}/m = 0.0828$, $\tau_{221}/m = 0.250$ and $\tau_{222}/m = 0.422$. We then determine the three unknown amplitudes and three unknown phases of the three QNMs by imposing the continuity of the frequency $\omega_{\rm D2}$, Eq. (23), the wave and its first five derivatives at $t = t_{\rm end}$. We note that this matching procedure is rather sensitive to the time of matching because the frequency is increasing very quickly around $t_{\rm end}$. In Fig. 21 we compare the frequency and the inspiral-(plunge)-merger–ring-down wave $\mathrm{Re}[_{-2}C_{22}]$ of the EOB model with the NR results for the case $d = 16$. The EOB ring-down frequency is computed from Eq. (23) where we used in $\mathrm{Im}[_{-2}C_{22}]$ the same three amplitudes and three phases of $\mathrm{Re}[_{-2}C_{22}]$. Were we using in $\mathrm{Im}[_{-2}C_{22}]$ the three amplitudes and phases obtained by matching it at $t_{\rm end}$, we would not obtain a good result. This is due to numerical errors introduced by matching separately $\mathrm{Re}[_{-2}C_{22}]$ and $\mathrm{Im}[_{-2}C_{22}]$ at $t_{\rm end}$.

As seen in Fig. 21, by matching the fundamental QNM and the first two overtones, the frequency transition becomes smoother, but nevertheless it differs from the NR frequency ω_λ. As we shall see in the next section, this effective way of including a short in time, but spread in frequency, merger phase, can mimic the frequency spread of the power spectrum of the NR waves, though with a slightly different power law.

Analytic matching to QNMs ringing

(Nagar, Damour, Tartaglia '06
Damour, Nagar '06)

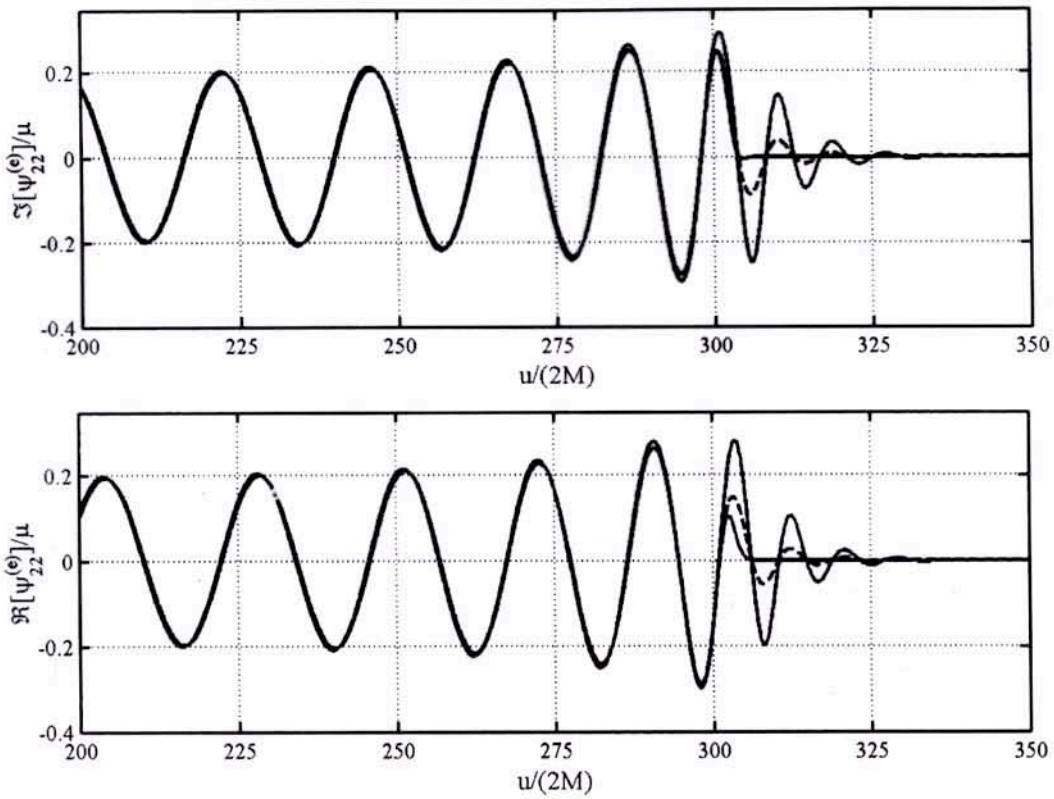

OCT06/

a_Idt_inf._eps

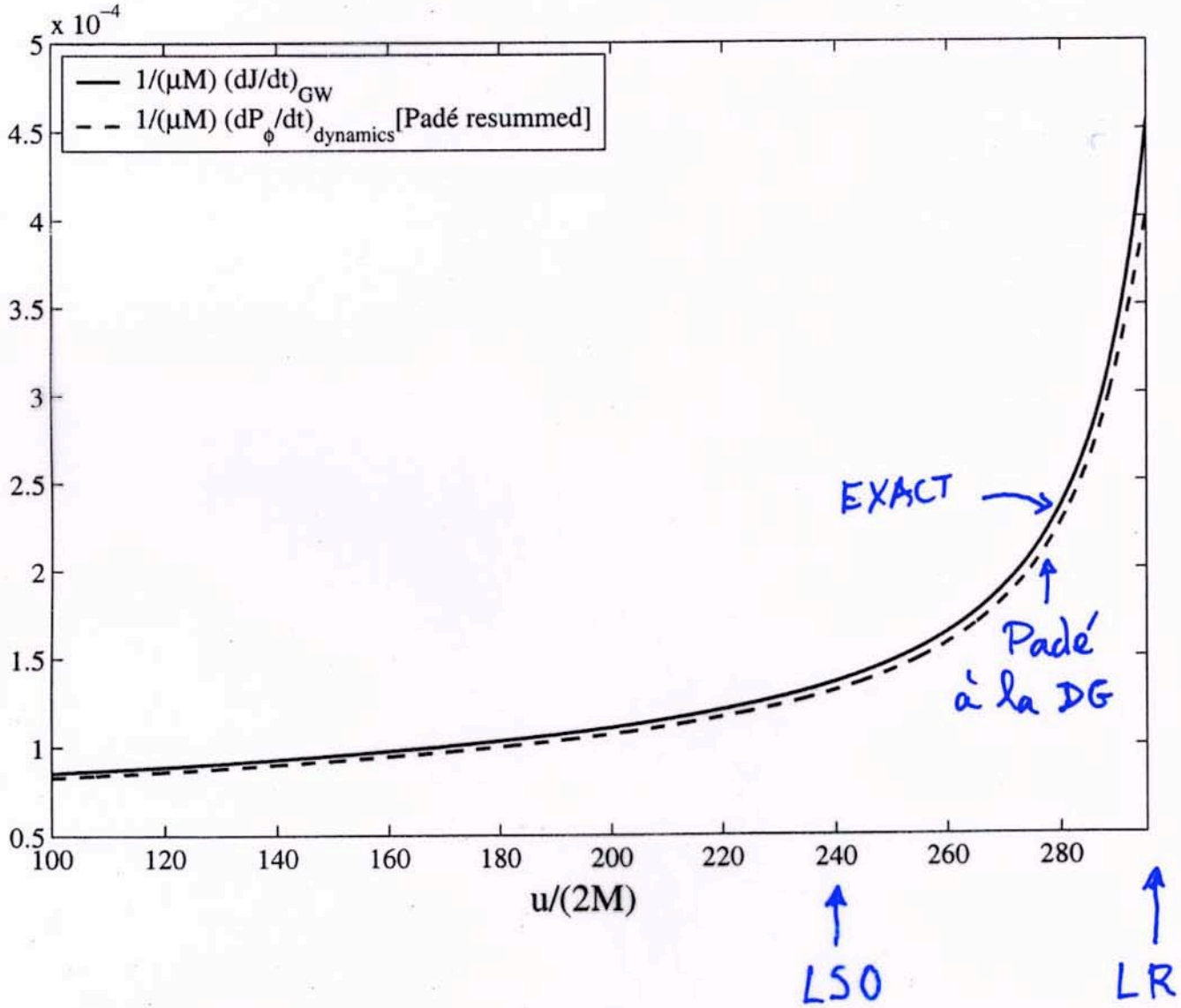

Phase : COMPARING ANALYTICAL AND NUMERICAL

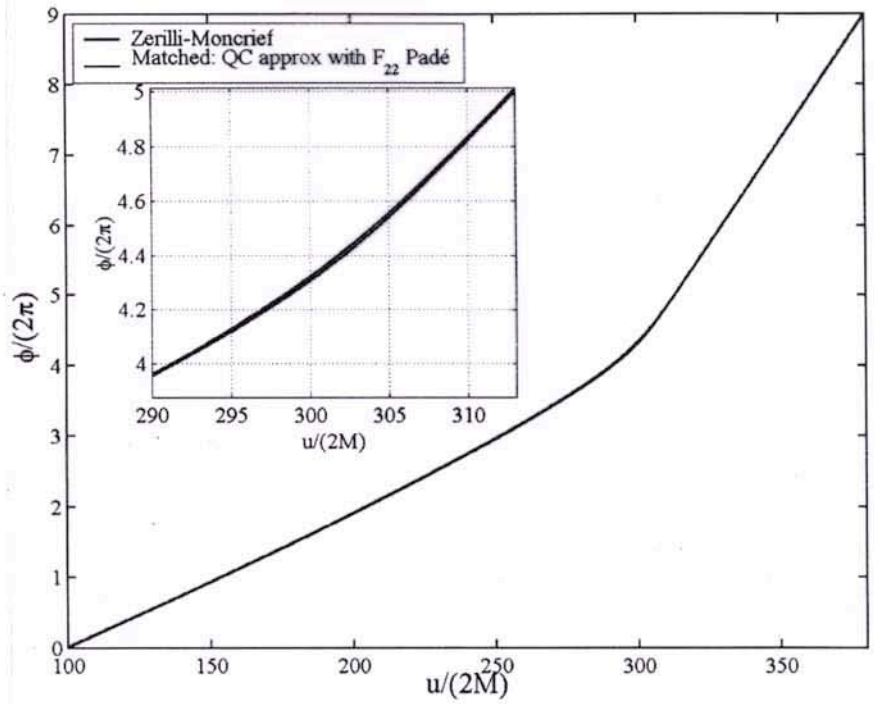

$\Delta\frac{\phi}{2\pi} < 1\%$ OF CYCLE

Analytic matching to QNMs ringing : INSTANTANEOUS GW FREQUENCY

Match to 5 (positive ω) QNMs

$$\Psi_{22}^{QNM} = \sum_{n=0}^{N} C_n e^{-\sigma_n^+ t}$$

$$\sigma_n^{\pm} = \alpha_n \pm i\omega_n$$

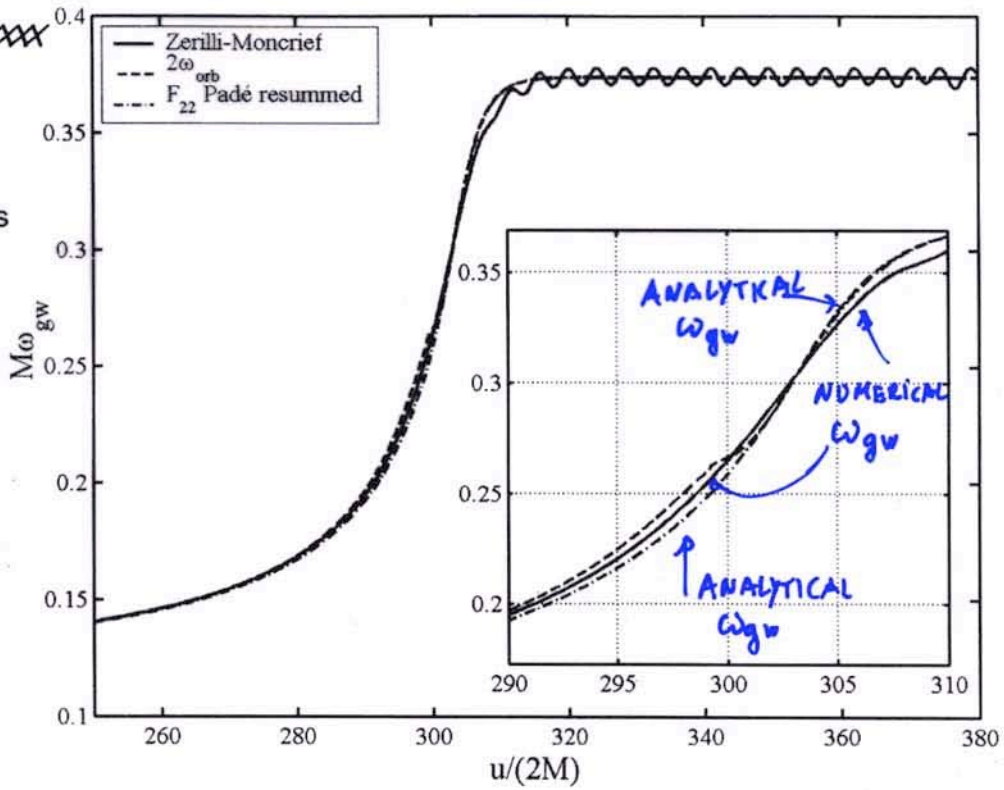

CONCLUSIONS

- IT IS IMPORTANT TO HAVE A SYNERGY BETWEEN ANALYTICAL AND NUMERICAL APPROACHES

- THE EFFECTIVE ONE BODY APPROACH, AFTER COMPARISON/FITTING/IMPROVEMENT, MAY PROVIDE AN EFFICIENT WAY OF BUILDING ACCURATE GW TEMPLATES FOR COALESCING BINARY BLACK HOLES WITH ARBITRARY $m_1, m_2, \vec{S}_1, \vec{S}_2$, eccentricity, $\vec{L}$, ...